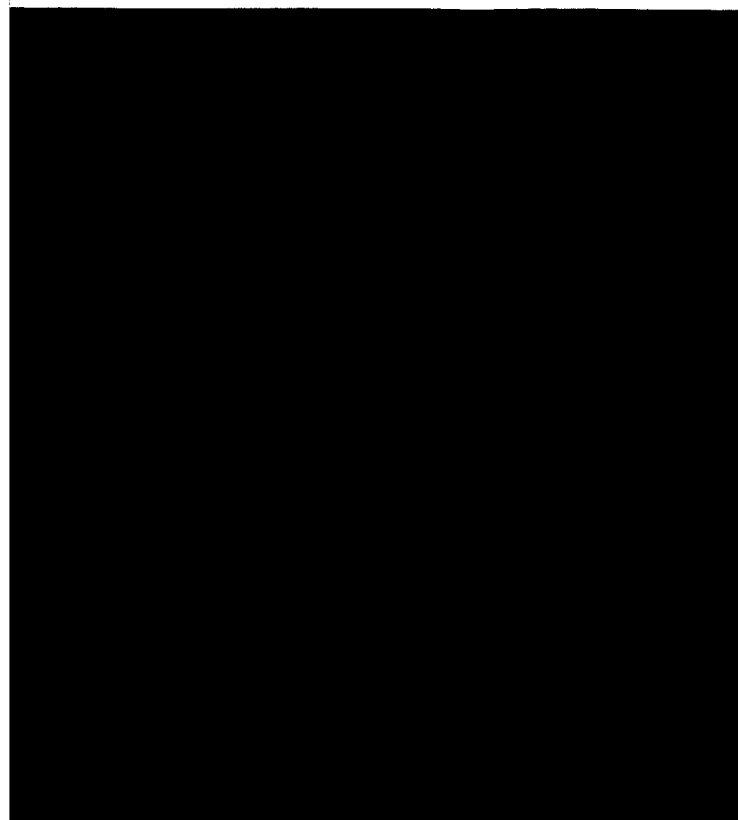


KINEMATIC STUDIES OF EARLY TYPE STARS.
I. PHOTOMETRIC SURVEY, SPACE MOTIONS, AND
COMPARISON WITH RADIO OBSERVATIONS

42P

163 22952

Code None



V. C. Rubin

Georgetown College Observatory
Washington, D. C.

J. Burley

Goddard Space Flight Center
Greenbelt, Maryland

A. Kiasatpoor, B. Klock, G. Pease, E. Rutscheidt and C. Smith

Georgetown College Observatory
Washington, D. C.

Kinematic Studies of Early-Type Stars. I. Photometric Survey, Space Motions, and Comparison with Radio Observations

VERA C. RUBIN

Georgetown College Observatory, Washington, D. C.

JAYLER BURLEY

Goddard Space Flight Center, NASA, Greenbelt, Maryland

AHMAD KIASATPOOR, BENNY KLOCK, GERALD PEASE, ERICH RUTSCHEIDT, AND CLAYTON SMITH
Georgetown College Observatory, Washington, D. C.

(Received August 2, 1962)

In order to compare the kinematic properties of early-type stars and gas in the solar vicinity, a catalogue of O-B5 stars with published radial velocities and within 3 kpc of the sun has been prepared. For 1440 stars, radial velocities, apparent magnitudes, spectral classes, and $B-V$ or other color measures have been taken from the literature; spectroscopically calibrated distances, corrected for absorption, have been computed. With the stars grouped in 5° longitude zones, the distribution of stellar radial velocity within each zone is compared with the corresponding 21-cm line profile. There is general qualitative agreement between the stellar and radio radial-velocity distributions in most longitude zones. However, the range in radial velocities exhibited by the stars is often larger than that predicted by the radio model of the galaxy, to a distance of 3 kpc from the sun. This could be accounted for by a value of R_0 larger than the conventional value of $R_0 = 8.2$ kpc, and by random stellar motions of the order of 20 km/sec in one component. In some longitude zones systematic differences appear; in the third quadrant, the stellar radial velocities are more nega-

tive than the velocities observed for the gas, even after the application of a +10 km/sec correction to the Lick radial velocities.

For 898 stars, proper motions on the N30 system are available, and cylindrical velocity components with respect to the center of the galaxy are computed. From the components of motion circular about the center of the galaxy, a mean rotation curve is derived for the stellar component of the galaxy in the solar vicinity. For a distance from the center of the galaxy $R = 6$ kpc, the mean circular velocity is about 15 km/sec larger than the circular velocity adopted for the radio model. At $R \approx 8$ kpc, the stellar and gas rotation curves coincide. For $R > 8.5$ kpc, the stellar curve is flat, and does not decrease as is expected for Keplerian orbits.

The velocity component II radial from the center of the galaxy has a large scatter for individual stars. In the mean, the II vs R curve has a negative slope of about -5 km/sec per kpc. Stars toward the center show a velocity of recession from the center; stars with large R indicate a slight velocity of approach toward the center, for the conventional choice of solar motion. This agrees well with the expansion observed for interstellar hydrogen.

Author

circular motion have been found for the gas in the expanding arm of the galaxy at 3 kpc from the center (van Woerden, Rougoor, and Oort 1957). Similarly, systematic deviations of the radial velocities of early-type stars from the predicted Oort double sine function are found (see Feast and Thackeray 1958).

In view of the great interest in this question, it is worthwhile to investigate the kinematical properties of young stars in the solar vicinity, not merely from a study of their radial velocities, but from a study of their galactic space motions. This paper presents the results of an investigation of radial velocities and space motions of 1440 O-B5 stars, within 11° of the galactic plane, and within 3 kpc of the sun, which was undertaken to determine the variation of galactic motions of these stars.

Neither Blaauw's (1956) study of nearby O and B stars, nor Eggen's (1961) analysis of the motions of bright O and B stars contains stars at sufficient distances from the sun to study their motions as a function of distance from the center of the galaxy. Hence an extensive catalogue of O-B5 stars has been prepared, and is presented in Sec. II. For each star, a distance is calculated from photometric data which have been taken from the literature. Each of the 1440 stars has a published radial velocity; 898 of the stars have both color measures and published proper motions as well.

Section III contains a comparison of the radial-velocity distribution of these stars with the correspond-

I. INTRODUCTION

THIS paper presents the results of a study of the motions of early-type stars in the galactic disk and within 3 kpc of the sun. The work was undertaken to investigate the general question of whether the stars and gas in the solar vicinity exhibit similar motions. In particular, studies were made to determine (1) whether the radial-velocity distribution of these stars, as a function of longitude, is similar to the radial-velocity distribution exhibited by the 21-cm hydrogen emission; (2) whether the variation of the circular velocity about the center of the galaxy of these stars is similar to the rotation curve determined from 21-cm observations; and (3) whether these stars show a systematic motion radial from the center of the galaxy.

In recent years, rapid progress in deducing the structure and dynamics of the galaxy has come from 21-cm observations. With the assumption of circular orbits, radio astronomers have analyzed the radial velocity of interstellar hydrogen and deduced a rotation curve for the gaseous component of the galaxy (Kwee, Muller, and Westerhout 1954; Schmidt 1956). From optical studies, again assuming circular orbits, Munch and Munch (1960) and earlier observers (Mayall 1951; Bahng, Code, and Whitford 1957) have derived a rotation curve for the stellar component of the galaxy by resolving the observed radial velocities of distant stars into motions at right angles to the radius vector from the center to each star. Yet large-scale deviations from

ing 21-cm $H\alpha$ radial-velocity distribution. The stellar velocities are grouped by longitude zones and examined by a procedure which approximates the method used to analyze the 21-cm observations. The results are presented graphically.

The galactic space motions of 898 stars from the catalogue are analyzed in Sec. IV. From the adopted radial velocity and proper motion of each star, a circular component about the center of the galaxy and a component radial from the center is computed. In Sec. V, a rotation curve for the stellar component of our region of the galaxy is determined, and compared with the rotation curve for the gaseous component. Section VI contains a discussion of the variation of the component radial from the center of the galaxy, for these stars. Some general conclusions from this study are presented in Sec. VII.

II. CATALOGUE

In order to study the space motions of early-type stars, a catalogue of O-B5 stars has been prepared, using the best available radial velocities, proper motions, luminosity, and spectral classifications. From Wilson's (1953) General Catalogue of Stellar Radial Velocities (GCRV), a list of all O-B5 stars, $|b| < 11^\circ$, with radial velocities accurate to within ± 5 km/sec was compiled. Additional stars of known constant radial velocity, principally from Feast, Thackeray, and Wesselink (1955, 1957) and Fehrenbach and co-workers (Barbier and Boulon 1959; Boulon, Duflot, and Fehrenbach 1958; Boulon and Fehrenbach 1959; Duflot and Fehrenbach 1956, 1957) were added to the list. A total of about 1600 stars was obtained. The published literature was searched for visual magnitudes, MK spectral classifications, absolute magnitudes, and $B-V$ or other color measures. For each star $m_0 - M$ was formed; only 1440 stars with $m_0 - M \leq 12.6$ ($r \leq 3.3$ kpc) were retained. The limiting distance of about 3 kpc is chosen as an optimistic compromise between the distance to which results are of interest and the distance to which observational material is available. These stars, with photometric data and sources for each, comprise Table I. The numbered references in the final four columns refer to the list of sources at the end of the table.

A description of each column follows.

Col. 1: A running number for each star. An asterisk indicates that the star has a published proper motion and is contained in Table IV.

† Col. 2: The Wilson (1953) number of the star. Numbers in italics refer to the list of references at the end of Table I, and identify the source of radial velocity for stars not in GCRV.

Col. 3: The HD number where available. Otherwise, BD, AGK₂, CPD, GC, Aitken (A), Kapteyn Area (K), NGC (N), or IC (I) number.

Cols. 4 and 5: New galactic coordinates (l^{II}) and (b^{II}), computed with the pole $\alpha = 12^{\text{h}}49^{\text{m}}$, $\delta = +27^\circ 4$,

as adopted by the International Astronomical Union (Blaauw, Gum, Pawsey, and Westerhout 1959).

Cols. 6 and 7: α and δ , 1950.

Col. 8: Radial velocity ρ uncorrected for the solar motion, from GCRV or other source listed in Col. 2. For a few stars, the tabulated value is a mean of recent observations (Fehrenbach and co-workers, Evans, Menzies, and Stoy 1959) and GCRV. No correction has been applied to the Lick velocities (Feast and Thackeray 1958) in the table.

Col. 9: Visual apparent magnitude V , where possible. Other visual magnitudes have been assumed to be equivalent to the magnitude of the Johnson-Morgan system. Corrections for duplicity have been adopted for eight stars as follows:

Star number	188	277	352	402	410	545	681	1137
Δm (mag.)	+0.2	+0.7	+0.11	+0.6	+0.16	+0.61	+0.2	+0.2

P following the magnitude indicates a photographic magnitude; v refers to a variable.

Col. 10: Spectral classification, on the MK system when available. The few stars later than B5 are classified B5 or earlier in GCRV.

Col. 11: Absolute magnitude, most often from the calibration of early-type stars of Johnson and Iriarte (1958). For stars with no luminosity class, class V has been assumed, and the Johnson-Iriarte calibration adopted. These values are enclosed in parentheses. About 60 stars have absolute magnitudes taken from Petrie and co-workers (Petrie 1955, 1956; Petrie and Moyle 1956; Beals 1955). Although the calibration of Petrie differs from that of Johnson-Iriarte, no correction has been applied. A value of $M = -7.0$ has been used for Of stars (Kopylov 1959).

Col. 12: Visual absorption in magnitudes A_v , most often from $B-V$ measures. A value of 3 for the ratio of total to selective absorption has been assumed. Normal colors were taken from Johnson (1958). The following conversions (Morgan, Harris, and Johnson 1953; Feast and Thackeray 1958) were adopted for color measures not on the UBV system:

$$\begin{array}{ll} \text{Morgan, Code, Whitford; Stebbins} & B-V = 2.07C_1 + 0.30 \\ \text{Oosterhoff} & B-V = 1.107C_1 + 1.371 \end{array}$$

The entry $A_v = 0.0$ indicates that the computed value was negative, but always equal to 0.0 to one decimal place.

Col. 13: Distance modulus, computed from $m - M - A_v$. Where photometric data are missing for one star in a double, the distance modulus of the second star is enclosed in parentheses. For stars with no individual M or A_v values, but which are known members of a cluster, the cluster distances have been listed. A uniform correction of $+0.2$ has been used to convert photographic to visual apparent magnitude for those stars indicated by P in Col. 9. In all, 1162 stars have computed distance moduli. The remaining stars have no absorption measures, and hence no listed distance

1. Barbier, M., and Boulon, J. 1959, *J. Obs.* **43**, 69.
2. Beer, A. 1961, *Monthly Notices Roy. Astron. Soc.* **123**, 191.
3. Bertiau, F. C., S. J. 1958, *Astrophys. J.* **128**, 533.
4. Blaauw, A. 1956, *ibid.* **123**, 408.
5. Blaauw, A., Hiltner, W. A., and Johnson, H. L. 1959, *ibid.* **130**, 69.
6. Boulon, J., Dufot, M., and Fehrenbach, Ch. 1958, *Publ. Obs. Haute-Provence* **4**, No. 34.
7. Boulon, J., and Fehrenbach, Ch. 1959, *ibid.* **4**, No. 55.
8. Buscombe, W., and Morris, P. M. 1960, *Monthly Notices Roy. Astron. Soc.* **121**, 263.
9. Canadian *Observer's Handbook* 1960, edited by R. J. Northcott (Royal Astronomical Society of Canada), p. 65.
10. Dufot, M., and Fehrenbach, Ch. 1956, *Publ. Obs. Haute-Provence* **3**, No. 49.
11. ——. 1957, *ibid.* **4**, No. 12.
12. Evans, D. S., Menzies, A., and Stoy, R. H. 1959, *Monthly Notices Roy. Astron. Soc.* **119**, 638.
13. Feast, M. W. 1957, *ibid.* **117**, 193.
14. ——. 1958, *ibid.* **118**, 618.
15. Feast, M. W., Thackeray, A. D., and Wesselink, A. J. 1955, *Mem. Roy. Astron. Soc.* **LXVII**, 51.
16. ——. 1957, *LXVIII*, 1.
17. Hiltner, W. A. 1956, *Astrophys. J. Suppl.* **2**, 389.
18. Hiltner, W. A., and Iriarte, B. 1955, *Astrophys. J.* **122**, 185.
19. Hiltner, W. A., and Johnson, H. L. 1956, *ibid.* **124**, 367.
20. Hoffeit, D. 1956, *ibid.* **124**, 61.
21. Hogg, H. S. 1959, *Handbuch der Physik*, edited by S. Flugge (Springer-Verlag, Berlin), Vol. LIII, p. 129.
22. Johnson, H. L. 1958, *Lowell Obs. Bull.* **4**, 37.
23. ——. 1960, *Astrophys. J.* **131**, 620.
24. Johnson, H. L., Hoag, A. A., Iriarte, B., Mitchell, R. I., and Hallam, K. L. 1961, *Lowell Obs. Bull.* **5**, 133.
25. Johnson, H. L., and Iriarte, B. 1958, *ibid.* **4**, 47.
26. Reference 25. Luminosity class V has been assumed.
27. Johnson, H. L., and Morgan, W. W. 1953, *Astrophys. J.* **115**, 313.
28. Kopylov, I. M. 1958, *Crimson Obs. Publ.* **XX**, 156.
29. ——. 1959, *Ann. d'Astrophys. Suppl.* **8**, 41.
30. McCuskey, S. W. 1956, *Astrophys. J. Suppl.* **2**, 298.
31. Meadows, A. J. 1961, *Monthly Notices Roy. Astron. Soc.* **123**, 81.
32. Mendoza, E. E. 1958, *Astrophys. J.* **128**, 207.
33. Reference 32. Known low-luminosity star; absolute magnitude has been determined from 32.
34. Reference 32. Luminosity class V assumed; absolute magnitude determined from 32.
35. Morgan, W. W. 1951, *Publ. Obs. Univ. Mich.* **10**, 33.
36. Morgan, W. W., Code, A. D., and Whitford, A. E. 1955, *Astrophys. J. Suppl.* **2**, 41.
37. Morgan, W. W., Whitford, A. E., and Code, A. D. 1953, *Astrophys. J.* **118**, 318.
38. Morris, P. M. 1961, *Monthly Notices Roy. Astron. Soc.* **122**, 325.
39. Munch, L. 1952, *Bol. Tonansinida y Tac.* **2**, 1.
40. Numerova, A. B. 1958, *Crimson Obs. Publ.* **XIX**, 189.
41. Oosterhoff, P. Th. 1951, *Bull. Astron. Inst. Neth.* **XI**, 299.
42. Petrie, R. M. 1955, *Publ. Dominion Astrophys. Obs.* **IX**, 297.
43. ——. 1955, *ibid.* **IX**, 251.
44. ——. 1956, *Vistas in Astronomy*, edited by A. Beer (Pergamon Press, London and New York), Vol. II, p. 1346.
45. Petrie, R. M., and Moyle, B. N. 1956, *Publ. Dominion Astrophys. Obs.* **X**, 287.
46. Popper, D. M. 1944, *Astrophys. J.* **100**, 94.
47. Roberts, M. S. 1962, *Astron. J.* **67**, 79.
48. Roman, N. G. 1951, *Astrophys. J.* **114**, 492.
49. Schmidt-Kaler, Th. Z. *Astrophys.* **53**, 1.
50. Seydel, C. K., and Popper, D. M. 1941, *Astrophys. J.* **93**, 461. For conversion to MK spectral class, see reference 46.
51. Sharpless, S. (unpublished).
52. Slettebak, A. 1955, *Astrophys. J.* **121**, 653.
53. Smith, E. van P. 1956, *ibid.* **124**, 43.
54. Stebbins, J., Huffer, C. M., and Whitford, A. E. 1940, *ibid.* **91**, 20.
55. Stoy, R. H. 1961, *Cape Memo.* **12**, Royal Obs., Cape of Good Hope.
56. de Vaucouleurs, A. 1957, *Monthly Notices Roy. Astron. Soc.* **117**, 449.
57. Walker, M. F. 1956, *Astrophys. J. Suppl.* **2**, 365.
58. Wilson, R. E. *General Catalogue of Stellar Radial Velocities* (Carnegie Institution of Washington, Washington, D. C.).
59. Woods, M. L. 1955, *Mem. Commonwealth Obs. Mt. Stromlo* **3**, 1.
60. Beals, C. S. 1955, *Publ. Dominion Astrophys. Obs.* **IX**, 1.

moduli; these stars will be within 3 kpc (unless, in a few cases, they are supergiants). With this possible exception, all 1440 stars in Table I have $m_0 - M \leq 12^m 6$.

Cols. 14, 15, 16, and 17: Sources for m , Spectral type, M , and A_v . The numbers refer to the references following the table. In cases where several values are available for one entry, preference is given, in general, to the most recent work.

For many stars, $m_0 - M$ in Table I does not agree exactly with $m_0 - M$ published by the original authors (for example Hiltner 1956; Oosterhoff 1951). This is due to our use of the recent Johnson-Iriarte calibration, rather than retaining the older calibration used by the observer. This fact, plus Stoy's (1961) recent publication of photometric data of southern stars on the *UBV* system, has substantially added to the uniformity of the data in Table I.

The intrinsic luminosities of the stars in Table I range from $M = -7^m 3$ for a supergiant to $M = -1^m 0$ for a B5V star. Hence a high-luminosity star with $m = 7$ will be too distant for inclusion, while a low-luminosity B5 star with $m = 11$ could be included. The radial-velocity observations cannot be considered complete even to $m = 7$, although some 10th-mag. stars are included. This means that while many supergiant stars at about 3 kpc are contained in this sample, no low-luminosity stars at 3 kpc have observed radial velocities. Indeed, the limiting distance of completeness for the low-luminosity stars must be within 500 pc, a distance which is hardly of galactic dimensions.

The distribution of spectral classes of these stars is listed in Table II. There are 281 stars with luminosity classes I, II, and III.

It is possible to estimate by several methods the total number of O-B5 stars within 3 kpc of the sun,

if we extrapolate from the number in the immediate solar vicinity. From the density of O, B, and A stars in the solar neighborhood (Schmidt 1956), a total of 15 000 O and B stars would be expected within 3 kpc, if the ratio of A stars to O and B stars is about 1000 to 1. This same number is predicted by the study of Blaauw (1956) from the 500 OB stars observed within 600 pc of the sun. From Roberts' (1957) estimate of the total number of early-type stars in the galaxy, about 7×10^4 OB stars are within 3 kpc of the sun, or 50 times the number of stars in Table I.

From a comparison of the number of OB stars in a small region of the Hamburg-Warner and Swasey atlas (Hardorp, Rohlfs, Slettebak, and Stock 1959) with the number of stars in Table I in the same region, it appears that about 6 to 10 times as many stars appear in the Hamburg work. This atlas, complete to $m_{pg} \approx 13$, should contain most of the OB stars within 3 kpc. From these various estimates, we conclude conservatively that perhaps 5% of all O-B5 stars within 3 kpc of the sun are contained in Table I.

Finally, we may estimate the completeness from Table I itself. In the table, there are 400 stars with $r \leq 500$ pc. If we assume that the table is essentially complete to this distance, then 15 000 stars would be expected to a distance 6 times as far. This is about 10 times the total number of stars in this study.

The projection on the galactic plane of the 1162 stars with computed values of $m_0 - M$ is shown in Fig. 1. The sun is in the middle; the concentric circles mark distances of 1, 2, and 3 kpc from the sun. The arcs indicate distance from the center of the galaxy, for an assumed value of $R_0 = 8.2$ kpc for the distance from the sun to the center.

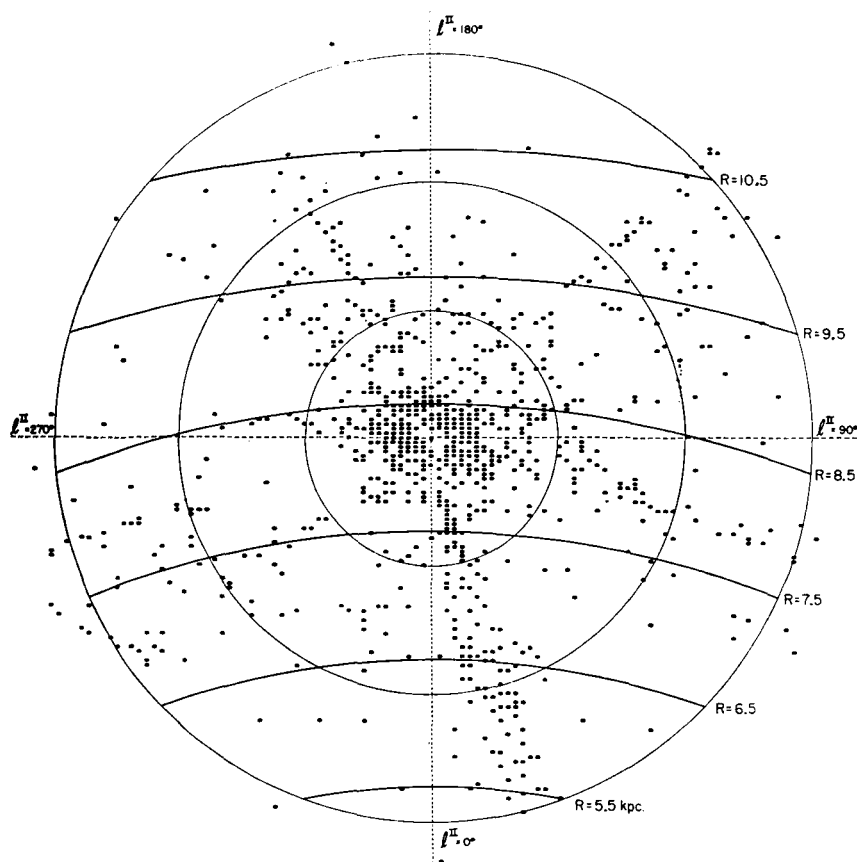


FIG. 1. The projection on the galactic plane of 1162 O-B5 stars with computed $m_0 - M$. Some points represent more than one star. The sun is at the middle; the concentric circles represent distances of 1, 2, and 3 kpc from the sun. The arcs indicate distance from the center of the galaxy, for $R_0 = 8.2$ kpc. The original plot was made from Table I by an IBM 7090.

Clearly, it is not easy to discern outlines of spiral structure from such a drawing alone. Whether the open lanes are real, due to observational selection, or due to absorbing matter in these directions is not known. However, there is a qualitative coincidence between the open lanes in Fig. 1, and the regions of maximum H I density in the Leiden surveys (Muller and Westerhout 1957; Schmidt 1957). The regions of greatest hydrogen density according to Schmidt (1957, Plate B) are at $\ell^{\text{II}} = 145^\circ$ and 155° , in the direction of the Perseus arm (Bok 1959). In Fig. 1, very few stars appear in the general region of the Perseus arm. Secondary maxima in the hydrogen density occur at $\ell^{\text{II}} = 45^\circ, 225^\circ, 240^\circ, 285^\circ$, and 320° . In most of these directions there is a marked absence of stars in Fig. 1. Beer (1961), in noting a similar anticorrelation between hydrogen density and early-type stars, has concluded that in regions of low gas density, star formation has depleted the gas. Significant amounts of gas would then be found only where there are few young stars.

A more simple explanation can actually suffice: in regions of maximum hydrogen density, the visual absorption is so great that giant O and B stars at 3 kpc are too faint for most observing programs. Toward $\ell^{\text{II}} = 146^\circ$, the total photographic absorption at $r = 1$ kpc is already $2^m 3$ (McCuskey 1956); the limiting magni-

tude of observation is thus effectively decreased at least one magnitude with respect to regions with $\ell^{\text{II}} < 130^\circ$. Detailed studies of faint OB stars at longitudes corresponding to the directions of maximum hydrogen density will be necessary to determine if spiral arms in our galaxy are marked by early-type stars, gas, and dust, or a combination of both stars and interstellar material. The Hamburg-Warner and Swasey program of observations of luminous stars in the northern Milky Way (Hardorp *et al.* 1959; Stock, Nassau, and Stephenson 1960) should make such studies possible.

The most notable concentrations of stars in Fig. 1 occur toward $\ell^{\text{II}} = 15^\circ$, the extension of the Sagittarius arm; toward $\ell^{\text{II}} = 200^\circ$, the Orion spur; and toward

TABLE II. Distribution of spectral classes for stars in Table I.

Spectral class	Number of stars	Number with computed $m_0 - M$
O	133	127
B0	175	170
B1	174	163
B2	224	199
B3	363	268
B4	69	30
B5	277	181
Bp, Be, later than B5	25	24

$\ell^{\text{II}} = 300^\circ$, the Carina-Cygnus arm. There is general agreement with the drawings of Bok (1959) and van de Hulst (1958). From this sample of stars alone, little evidence is found for placing the sun at the inner edge of a spiral arm.

When all B3 and later-type stars are deleted from Fig. 1, only the region within 500 pc of the sun is altered significantly. No clearer outline of galactic structure emerges, however.

III. RADIAL VELOCITIES

Rapid progress has been made in recent years in the study of the structure of our galaxy, from the analysis of the radial velocities of the 21-cm $H\alpha$ emission line. On the assumption that the average motion of matter in the galactic disk is perpendicular to the radius vector from the center, and that the velocity of rotation is independent of the position angle of this radius vector, the relation between the mean radial velocity ρ , longitude ℓ^{II} , and angular velocity $\omega(R)$, follows directly from geometrical considerations:

$$\rho = R_0 [\omega(R) - \omega_0] \sin \ell^{\text{II}}, \quad (1)$$

where R_0 is the distance from the sun to the center and ω_0 is the angular velocity in the vicinity of the sun. For adopted values of R_0 , ω_0 , and the variation of $\omega(R)$ with R , the analysis of the 21-cm line profile at a given longitude makes it possible to associate an observed radial velocity with a corresponding distance from the center of the galaxy.

Operationally, the radio astronomer looks along a wide-angle line of sight, and records the integrated intensity of 21-cm emission at all distances along this line as a function of radial velocity. In contrast, the optical astronomer observes radial velocities for individual stars at known (or approximately known) distances, at all longitudes. Because of the differences inherent in the observing and analyzing procedures, it is not surprising that it is difficult to relate the motions of the stars to the motions of the gas. Since the radio observations record a range in radial velocity, it is risky to attempt to identify any one hump in the radio line profile with an optical feature. Yet the great interest in determining whether the motions of the gas and stars are similar makes it worthwhile to devise some method of comparison which will be meaningful.

In an attempt to analyze the stellar data by a method approximating that used for radio observations, the following procedure is adopted. The stars in Table I are divided into 5° zones, each zone centered at a longitude for which a 21-cm line profile is available. The distribution of stellar radial velocities in each zone is compared with the corresponding 21-cm line profile. The zone width adopted, about twice the beamwidth of the Dutch receiver, was chosen so as to include a sufficient number of stars. In the case of radio observations the intensity received at the antenna from two

similar sources at different distances would differ, the nearer being more intense. In the present study, however, each star is given unit weight. For the stellar sample, the observational selection should compensate, to some degree, for the natural weighting in the radio observations.

The distribution of the stellar radial velocities from Table I is shown in Fig. 2. The midpoint of each longitude zone and the number of stars in each zone are listed in columns 1 and 2. The remaining columns tabulate the number of stars within each 10 km/sec radial-velocity interval; the midpoint of the velocity interval is shown at the head of each column. No correction for solar motion has been applied. Each Lick radial velocity for stars $m \geq 6.5$ has been corrected +10 km/sec, as suggested by Feast and Thackeray (1958). For stars with a velocity in GCRV which is a weighted mean of several observations, including Lick, the Lick observations have been corrected +10 km/sec and a new weighted mean computed. A total of 455 Lick (or means including Lick) stars are included in the 1440 stars.

The sine curve superimposed in the tabulated values of Fig. 2 represents the zero point of radial velocity, after correction for the local solar motion of 20 km/sec toward $\alpha = 270^\circ$, $\delta = +30^\circ$ ($\dot{x}_0 = +10.5$, $\dot{y}_0 = +15$, $\dot{z}_0 = +7$ km/sec). This value was chosen to conform to the value used in reducing the radio observations. The (approximate) double sine in Fig. 2 marks the limits of the radial velocities predicted by Eq. (1) for the neutral hydrogen to a distance of 3 kpc, with $R_0 = 8.2$ kpc, $\omega_0 = 26.4$ km/sec per kpc, and the variation of $\omega(R)$ with R as given by Schmidt (1956). If the motion of the stellar component of the galaxy is similar to that of the gaseous component, this double sine should also mark the limits of the stellar radial velocities. Radial velocities in excess are due to either random motions, systematic noncircular motions, or errors in the adopted parameters. However, because in most longitude zones the stellar sample includes no stars as distant as 3 kpc, the amplitude of variation should actually be smaller than that shown by the curve.

These radial velocity distributions are plotted as histograms in Fig. 3. The number of stars in each 10 km/sec interval, corrected for the local solar motion, is shown for 28 longitude zones. In some cases, the sum of two adjacent zones has been plotted. The bar at the base of each histogram indicates the radial-velocity range predicted for the radio model of the galaxy, to a distance of 3 kpc from the sun; the black portion of the bar is the velocity range to a distance of 1.5 kpc. Superimposed on each histogram is that part of the corresponding 21-cm line profile which covers the same radial-velocity interval, corrected only for the local solar motion. For $0^\circ \leq \ell^{\text{II}} \leq 242^\circ$, the line profiles come from Muller and Westerhout (1957); for $255^\circ \leq \ell^{\text{II}} \leq 341^\circ$ they are from Kerr, Hindman, and Gum (1959).

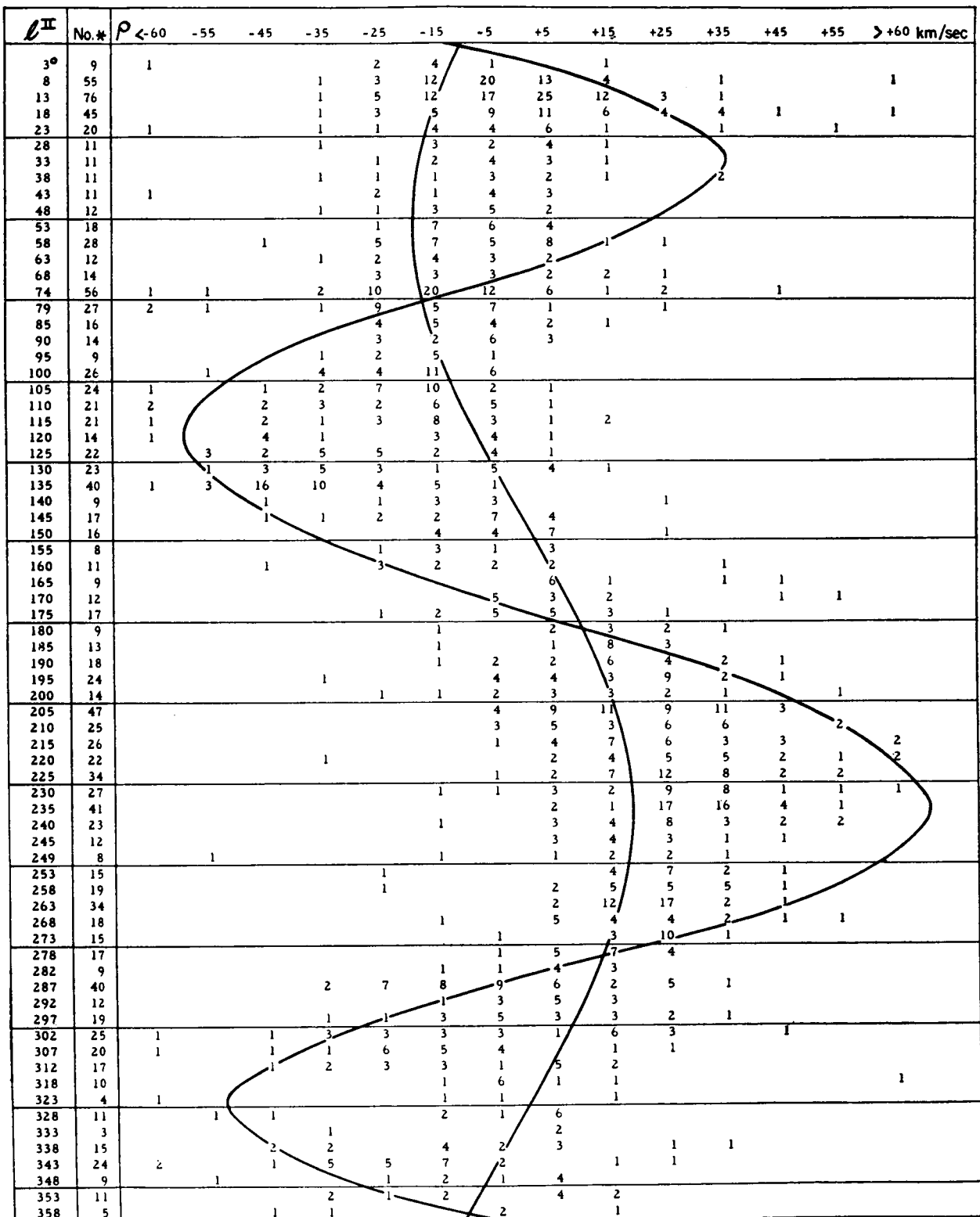


FIG. 2. The distribution of stellar radial velocities from Table I, by longitude zones. The midpoint of each radial velocity interval is shown at the top of each column. The sine curve represents the zero point of radial velocity after correction for the local solar motion. The (approximate) double sine marks the limits of the radial velocities predicted by the radio model of the galaxy for matter at a distance of 3 kpc from the sun.

At each longitude, the stellar and radio radial velocities should be compared only over the range predicted by Eq. (1), indicated by the bar in each zone. In the radio line profiles, radial velocities in excess of those predicted are assumed to come from clouds at distances greater than $r=3$ kpc.

The comparison of the line profiles and the optical histograms can be only qualitative, at best; we are not comparing areas under the curves but only gross features. For small l^{II} , although the histograms have well-defined maxima, the range in radial velocity is considerably greater than predicted. The width of the 21-cm line profiles is also greater, but this is attributed to emission from clouds at great distances from the sun. In the profile at $l^{\text{II}}=26^\circ$, for example, the maximum at $\rho=-35$ km/sec is placed at about $r=17$ kpc, i.e., beyond the center of the galaxy, because at this longitude all radial velocities within 3 kpc of the sun should be positive. In the stellar case, with distances of the stars known, the excess radial velocities and the negative tails for $l^{\text{II}}<79^\circ$ give some idea of the random stellar velocities; peculiar motions of 20 km/sec in one component must be common if we adopt the radio model of the galaxy.

In general, the agreement between the radio and the stellar data is reasonable, for $l^{\text{II}}<70^\circ$, with the exception that the stellar velocities cover a greater range than that expected from Eq. (1).

At $l^{\text{II}}=79^\circ$, clouds with $r=3$ kpc are at a distance $R=8.2$ kpc from the center of the galaxy, so $\omega(R)-\omega_0=0$. The optical radial-velocity distribution at this longitude thus reflects only the random motions of the stars. However, the observed radial-velocity spread of over 50 km/sec at this longitude is well over twice the random cloud velocity of 6 km/sec adopted by Westerhout (1957). A curious fact is that this zone contains exceptionally young stars: 6 of the 27 stars in the zone are O9 or earlier, only 4 are B3 or later. The 13 stars with $\rho \leq -5$ km/sec contain only one star later than B1.5. Thus the youngest stars, which might be expected to reflect the motions of the gas from which they have recently formed, are moving with velocities considerably in excess of the adopted random gas velocity. However, the apparent random motions of the order of 20 km/sec indicated by the stars in this zone ($l^{\text{II}}=79^\circ$) are close to the value $\sigma=14.8 \pm 2.2$ km/sec computed by Feast and Thackeray (1958) from their study of 150 O and B stars.

In the longitude zones $87^\circ \leq l^{\text{II}} \leq 147^\circ$, the second maximum in the radio profiles, at about $\rho=-50$ km/sec, is due to hydrogen in the Perseus arm. Similar secondary peaks are lacking in the stellar sample. In these regions especially, only velocities included in the darkened portion of the bar should be considered, because of the absence of stars beyond about $r=1.5$ kpc. Here, too, the range in stellar velocities exceeds the predicted range.

In the third quadrant, the stellar radial velocities are excessively negative, with respect to the radio observations and the predicted velocities, even though a correction of +10 km/sec has been applied to the Lick observations. If the circular velocity of these stars is greater than that adopted for the radio model, then excess negative velocities would be observed. Corresponding excess positive velocities would be expected in the second quadrant, but the lack of distant stars in this quadrant makes the comparison impossible at this time.

For $l^{\text{II}} > 270^\circ$, there is general agreement between the main features of the histograms and the radio line profiles. The large positive tails in both the radio and the optical cases have signs opposite to that expected for nearby objects in the fourth quadrant.

From this general qualitative comparison it appears that the distributions of stellar radial velocities in the galactic plane are not dissimilar to the radial velocity distributions of the 21-cm line profiles. This was to be expected, perhaps, for the adopted procedure is insensitive to small-scale irregularities. However, in

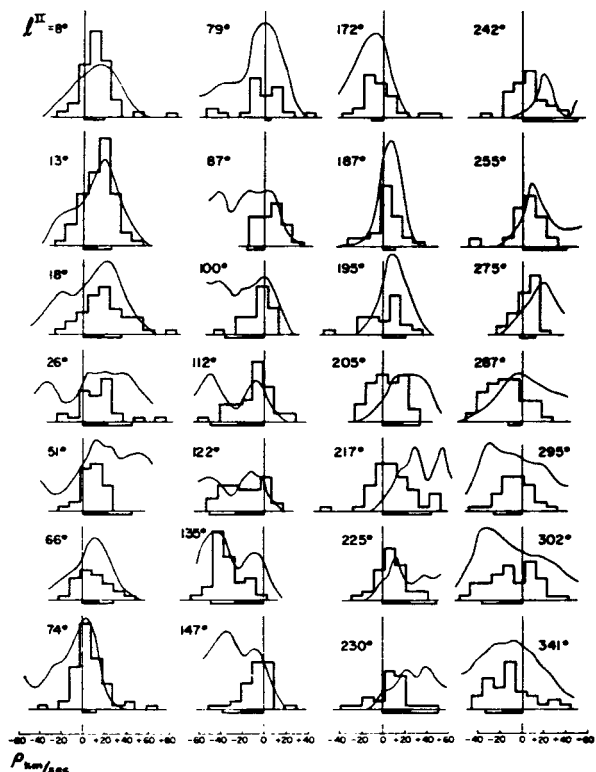


FIG. 3. A comparison, by longitude zones, of the distribution of stellar radial velocities with the corresponding 21-cm line profile. The number of stars in each 10 km/sec velocity interval is shown by the histogram; the radial-velocity scale is at the base of each column. Both stellar and radio radial velocities have been corrected for the local solar motion. The bar at the base of each histogram indicates the predicted range of radial velocities for matter within 3 kpc of the sun, on the usual radio model of the galaxy. The blackened portion of each bar represents the predicted velocity range to a distance of $r=1.5$ kpc.

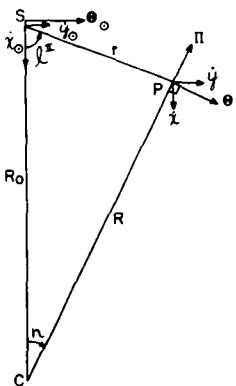


FIG. 4. The kinematical relations between the sun S, the center of the galaxy C, and a star at P. The sun has rectangular velocity components \dot{x}_0 and \dot{y}_0 in the galactic plane. The rotational velocity about the center of the galaxy at the position of the sun is Θ_0 . The star at P has rectangular velocity components \dot{x} and \dot{y} . For P, the cylindrical velocity components about the center of the galaxy are given by Θ , at right angles to the line CP and positive in the direction of rotation; and Π , radial along the line CP and positive outward.

many directions the stellar radial velocities exceed those predicted by the usual radio model of the galaxy. Two explanations could account for this. It is likely that random stellar velocities are larger than random motions assumed for the clouds. Unfortunately, the random motions of both the stars and of the gas clouds are not known with any certainty. In the stellar case, the large motions of O and B stars in associations are attributed by Blaauw (1956 and references therein) to an expansion from newly formed associations. Petrie (1958) and Woolley and Eggen (1958) conclude that such motions are random, rather than systematic. In either case, however, it would be expected that in some directions in the galactic plane, large ranges in stellar radial velocities would be observed. Whether, in such regions, a corresponding larger velocity of the $H\alpha$ clouds is to be expected depends on the model one adopts for the formation of stars and associations. An excellent review of this problem has been given by Kahn (1960) and is omitted here.

A second explanation for the spread in the observed stellar radial velocities is that the distance from the center of the galaxy to the sun is greater than 8.2 kpc (Weaver 1961). If R_0 is increased to $R_0=10$ kpc, but $\omega(R)-\omega_0$ is not altered, then the absolute value of the predicted radial velocity at each longitude [Eq. (1)] would be increased by about 25%; each bar in Fig. 3 would be lengthened by 25%. This correction would not account for the long tails of the distributions, with signs opposite to those predicted, nor would it improve the agreement in the directions where $\omega(R)-\omega_0$ is small. In many directions, however, increasing R_0 would improve the agreement between the stellar and the 21-cm observations.

The double sine in Fig. 2 has been drawn for $R_0=8.2$ kpc, $r=3$ kpc. For a value of $R_0=10$ kpc, the same

curve would indicate the predicted radial velocity for matter at $r=2.3$ kpc. This distance is a reasonable one for the stellar sample; only 10% of these stars have $r>2.3$ kpc. Hence the curve for $R_0=10$ kpc, $r=2.3$ kpc should represent fairly well the limits of the radial-velocity distribution.

IV. GALACTIC SPACE MOTIONS

Munch and Munch (1960) have recently deduced a rotation curve for the inner parts of the galaxy from the radial velocities of 18 distant early-type stars, assuming circular orbits about the galactic center. Each observed radial velocity was resolved into a velocity at right angles to the radius vector from the center to the star, and the variation of this rotational velocity was examined as a function of distance from the center. Toward the center of the galaxy, where the results are of most interest, the angle between the radial velocity and the circular component approaches 90° , so any random stellar motion or motion of the star radial from the center will be magnified and included in the circular component. While additional radial-velocity data will eliminate the influence of the random motions, systematic radial motions will continue to obscure the results.

It is possible to determine a rotation curve of the stellar component of the galaxy in the solar vicinity, from the space motions of early-type stars in the galactic disk, without assuming strictly circular motions. In this case, the proper motions as well as the radial velocities are employed. Even though the accuracy of the proper motions has long been a subject of debate, it should be possible to obtain meaningful results for a large sample of stars, barring large systematic errors in the proper motions.

In Fig. 4, a star near the galactic plane at P is at longitude l^{II} and distance r from the sun S. The center of the galaxy is at C; the distance from the sun to the center of the galaxy is R_0 , the distance from the center to the star is R . The sun is assumed to have known velocity components \dot{x}_0 , \dot{y}_0 , and \dot{z}_0 with respect to the local standard of rest: \dot{x}_0 in the direction $l^{\text{II}}=0^\circ$, $b^{\text{II}}=0^\circ$; \dot{y}_0 in the direction $l^{\text{II}}=90^\circ$, $b^{\text{II}}=0^\circ$; \dot{z}_0 in the direction $b^{\text{II}}=90^\circ$. In the vicinity of the sun, the rotational velocity about the center of the galaxy is given by $\Theta_0=\omega_0 R_0$.

For a star at P with observed proper motion and radial velocity, the tangential velocity components in longitude T_l , and latitude T_b , computed from the proper motion in longitude and latitude, are given by

$$T_l = \kappa r \mu_l'' \text{ km/sec}, \quad T_b = \kappa r \mu_b'' \text{ km/sec}; \quad \kappa = 4.74. \quad (2)$$

The space components in the galactic plane, corrected for the local solar motion and the rotational velocity

at the sun, are

$$\dot{x}_c = -T_1 \sin l^{\text{II}} - T_2 \cos l^{\text{II}} \sin b^{\text{II}} + \rho \cos l^{\text{II}} \cos b^{\text{II}} + \dot{x}_0, \quad (3)$$

$$\dot{y}_c = T_1 \cos l^{\text{II}} - T_2 \sin l^{\text{II}} \sin b^{\text{II}} + \rho \sin l^{\text{II}} \cos b^{\text{II}} + \dot{y}_0 + \Theta_0. \quad (4)$$

We now define a cylindrical velocity component system, centered at the center of the galaxy; Θ is the velocity component perpendicular to the radius vector from the center to the star, parallel to the galactic plane, and positive in the direction of rotation; Π is the component radial from the center of the galaxy, parallel to the galactic plane and positive outward; Z is the component perpendicular to the galactic plane. For the star at P , the Θ and Π components are

$$\Theta = \dot{x}_c \sin n + \dot{y}_c \cos n, \quad (5)$$

$$\Pi = -\dot{x}_c \cos n + \dot{y}_c \sin n, \quad (6)$$

where n is the galactocentric longitude of P , measured in the direction of rotation.

If P is in the galactic plane, \dot{x}_c and \dot{y}_c simplify, and Fig. 4 is a plane figure. If P is not in the galactic plane, then in Fig. 4, \dot{x}_c , \dot{y}_c , Θ , and Π are not in the plane of the page, but parallel to it. Equations (5) and (6) are exact; no approximation has been made in computing the Θ and Π components of each star.

Because of the greater accuracy in the linear velocity determined from radial-velocity observations than from the proper-motion observations, it is important to be able to estimate the probable error in each of the computed components. For a star in the direction of the center of the galaxy, the Π component is coincident with the radial-velocity component, so the probable error of Π for stars in this direction will not increase for increasing distance of the stars. The Θ component in this direction coincides with the proper-motion component, and hence its probable error will be larger for more distant stars. For a star near $l^{\text{II}} = 90^\circ$, the Θ component is coincident with the radial velocity and will be well determined. In addition, for any chosen distance R from the center of the galaxy, some stars will be near the sun, others will have $r \approx 3$ kpc. These latter stars will have less well determined Θ and Π components, and should be given less weight in the determination of mean Θ and mean Π for that value of R .

For these reasons, a probable error of each component has been computed for every star as follows. From Eqs. (3) and (4), for a star in the galactic plane, to first order in r/R ,

$$\dot{x}_c = -T_1 \sin l^{\text{II}} + \rho \cos l^{\text{II}} + \dot{x}_0, \quad (7)$$

$$\dot{y}_c = T_1 \cos l^{\text{II}} + \rho \sin l^{\text{II}} + \dot{y}_0 + \Theta_0, \quad (8)$$

$$\cos n = 1, \quad (9)$$

$$\sin n = (r/R) \sin l^{\text{II}}. \quad (10)$$

TABLE III. Proper-motion data for 898 O-B5 stars.

Source No.	Source	Number of stars	Probable error
1	Bertiau (1958)	30	± 0.003
2	Morgan (1956)	304	.003
3	Morgan (1952)	51	.003
4	<i>Yale Trans.</i> 24, 25, 26, 27	78	.004
5	<i>Cape Obs. Ann.</i> XVII, XVIII, XIX, XX	35	.007
6	General Cat. (Boss 1937)	211	.006
7	<i>Yale Trans.</i> 12-14; 16-22	185	.007
8	Reiz (1957)	3	.006
9	Morgan (1933)	1	± 0.006

Hence from (5) and (6),

$$\Theta = \dot{x}_c (r/R) \sin l^{\text{II}} + \dot{y}_c, \quad (11)$$

$$\Pi = -\dot{x}_c + \dot{y}_c (r/R) \sin l^{\text{II}}. \quad (12)$$

To a degree of approximation which is satisfactory for the error analysis, we write

$$\epsilon(\Theta) \approx \epsilon(\dot{y}_c), \quad (13)$$

$$\epsilon(\Pi) \approx \epsilon(-\dot{x}_c), \quad (14)$$

where ϵ represents the probable error of the quantity in parenthesis. Hence from (2), (8), (13), and the relation between m and r ,

$$\epsilon(\Theta) = \epsilon(T_1 \cos l^{\text{II}} + \rho \sin l^{\text{II}} + \dot{y}_0 + \Theta_0), \quad (15)$$

$$\epsilon(T_1) = \pm [\kappa^2 r^2 \epsilon^2(\mu_i) + \kappa^2 \mu_i^2 \epsilon^2(r)]^{\frac{1}{2}}, \quad (16)$$

$$\epsilon(r) = r [(\log_{10} 10)/5] \epsilon(m_0 - M). \quad (17)$$

Thus,

$$\epsilon(\Theta) = \pm \{ \kappa^2 r^2 \cos^2 l^{\text{II}} [\epsilon^2(\mu_i) + 0.21 \mu_i^2 \epsilon^2(m_0 - M)] + \sin^2 l^{\text{II}} \epsilon^2(\rho) \}^{\frac{1}{2}}. \quad (18)$$

For any star, the probable error of Θ involves two terms, one of which varies as $r \cos l^{\text{II}}$ times the probable error in the proper-motion observations, and will be the dominant term except when $\cos l^{\text{II}}$ is small. The second term varies as $\sin l^{\text{II}}$ times the probable error in the radial-velocity observations, and is not a function of distance of the star. In directions where $\cos l^{\text{II}}$ is small, $\epsilon(\Theta)$ will be small, in general; for stars with large r and $\cos l^{\text{II}} \approx 1$, $\epsilon(\Theta)$ will be large. At any given R , the stars with large probable errors should be given less weight in the formation of the mean Θ for that R .

Similarly, from Eqs. (2), (7), and (14),

$$\epsilon(\Pi) = \pm \{ \kappa^2 r^2 \sin^2 l^{\text{II}} [\epsilon^2(\mu_i) + 0.21 \mu_i^2 \epsilon^2(m_0 - M)] + \cos^2 l^{\text{II}} \epsilon^2(\rho) \}^{\frac{1}{2}}. \quad (19)$$

The error in the Π component will be smallest for $\cos l^{\text{II}} \approx \pm 1$, i.e., toward the center and anticenter.

For 898 stars with absorption measures and computed values of $m_0 - M$ in Table I, proper motions on the N30 system were obtained. The sources of the proper motions and the adopted probable error of each source are listed in Table III.

Proper motions not on the N30 system were converted to N30 by means of the tables given by Morgan (1952). Proper motions from sources 4, 5, 7, and 9 were first converted to the GC system by tables published in each source, then converted to N30. The correction to the precession recommended by Morgan and Oort (1951) has been applied.

For 898 proper-motion stars indicated by an asterisk in Table I, the Θ and II components and the probable errors of each have been computed on the NASA IBM 7090. The results of the calculations are contained in Table IV. A description of the table follows.

Cols. 1, 2, and 3: Star number, longitude (l^{II}), and radial velocity, repeated from Table I. The Lick radial velocities have not been corrected.

Cols. 4 and 5: Annual proper motion in right ascension μ_a and declination μ_b , on the N30 system, with the Morgan-Oort (1951) correction applied.

Cols. 6 and 7: Annual proper motion in galactic longitude μ_l and galactic latitude μ_b , based on the new galactic coordinates.

Col. 8: Distance from the sun to the star r computed from $m_0 - M$, Table I.

Col. 9: Distance from the center of the galaxy to the star R for $R_0 = 8.2$ kpc. A change in R_0 would change each computed R by the same amount, to first order in r/R .

Cols. 10 and 11: The tangential motion in longitude T_l and latitude T_b , in km/sec, not corrected for the local solar motion.

Cols. 12, 13, and 14: Components of space motion of the star, \dot{x} , \dot{y} , and \dot{z} , centered at the sun, uncorrected for solar motion. The axes are directed: \dot{x} toward $b^{II} = 0^\circ$, $b^{II} = 0^\circ$; \dot{y} toward $l^{II} = 90^\circ$, $b^{II} = 0^\circ$; \dot{z} toward $b^{II} = 90^\circ$.

Col. 15: The component of motion of the star at right angles to the radius vector from the center of the galaxy to the star Θ , computed from Eq. (5), minus the circular velocity at the sun. This is followed by the computed probable error of Θ , Eq. (18). Conventional values for the local solar motion and the rotational velocity at the sun were adopted: $\dot{x}_0 = +10.5$ km/sec, $\dot{y}_0 = +15$ km/sec, $\dot{z}_0 = +7$ km/sec, $\Theta_0 = 215$ km/sec (van de Hulst, Muller, and Oort 1954; these authors use $\Theta_0 = 216$ km/sec). The following probable errors of observation were adopted:

$$\begin{aligned}\epsilon(m_0 - M) &= \pm 0^m 3, \\ \epsilon(\rho) &= \pm 5 \text{ km/sec for 683 non-Lick stars}, \\ \epsilon(\rho) &= \pm 8 \text{ km/sec for 215 Lick stars}, \\ \epsilon(\mu_l) &\quad \text{from Table III.}\end{aligned}$$

Col. 16: The component of the motion of the star in the direction radial from the center of the galaxy, followed by the probable error. These quantities have been computed from Eqs. (6) and (19), with the parameters listed above.

Col. 17: The source of the proper motion; the numbers refer to Table III. Where two sources are listed, the mean of two published values has been adopted.

The formation of a rotation curve for the stellar component of the galaxy is discussed in the next section.

V. ROTATION CURVE

For each of the 898 stars in the solar vicinity, a Θ component of motion has been computed, without any assumption of circular orbits of the stars. However, in order to form from these values one mean curve, we must assume that it is meaningful to group all the stars at a given distance from the center of the galaxy into one mean point. This mean is then the value $\langle\Theta\rangle$ for that R .

The stars in Table IV were divided into 18 groups according to distance from the center of the galaxy. A weighted mean and its probable error, $\langle\Theta\rangle \pm \epsilon(\langle\Theta\rangle)$, was formed for each group, using the relation

$$\langle\Theta\rangle \pm \epsilon(\langle\Theta\rangle) = \frac{\sum w_i \Theta_i}{\sum w_i} \pm 0.6745 \left[\frac{\sum w_i (\Theta_i - \langle\Theta\rangle)^2}{(n-1) \sum w_i} \right]^{1/2}. \quad (20)$$

The weight corresponding to each value Θ_i is the inverse square of the computed probable error of Θ_i . The weighted mean and the probable error of the weighted mean is shown for each of the 18 distance groups in the lower drawing of Fig. 5; the values are listed in Table VI. Eight isolated stars closest to the center and the two most distant ones have not been included in the mean. The solid curve represents the rotation curve of the gaseous component of the galaxy, from Kwee, Muller, and Westerhout (1954) and Schmidt (1956).

For distances closer to the center of the galaxy than the sun, the rotation curve lies above the radio curve. This is similar to the results of Munch and Munch (1960) from the analysis of the radial velocities of 18 distant OB stars. For distances farther from the galactic center than the sun, the stellar velocities do not decrease as does the Schmidt curve, as is expected on the basis of Keplerian orbits.

At $R = 8.2$ kpc, the value of $\langle\Theta\rangle - \Theta_0$ is zero, for $\dot{y}_0 = +15$ km/sec. This implies that with respect to all stars in the ring $R = 8.2$ kpc in this sample, the sun is moving 15 km/sec faster than the mean rotational velocity at this distance.

It is important to investigate to what extent this computed rotation curve would be affected by systematic errors in the observed quantities. In this section we consider the effects of systematic observational errors in (a) the MK luminosity calibration; (b) the proper-motion system; (c) the radial velocities.

TABLE IV. Distances, radial velocities, proper motions, and galactic space motions for 898 O-B5 stars.

Star No. (1)	ℓ^{II} (2)	ρ km/sec (3)	μ_α 0.0000 (4)	μ_δ 0.0000 (5)	μ_1 0.0000 (6)	μ_2 0.0000 (7)	μ_3 0.0000 (8)	γ kpc (9)	R pc (10)	T_1 km/sec (11)	T_2 km/sec (12)	\dot{z} km/sec (13)	$\dot{\psi}$ km/sec (14)	\dot{s} km/sec (15)	$\Theta - \Theta_0$ km/sec (16)	Π km/sec (17)	Source $\mu_{\alpha, \delta}$ (18)
1	0°46	- 4	+00	-20	-17	-12	0.2	8.0	-16	-11	- 2	-16	-11	- 1 ± 4	- 8 ± 5	5 2	
2	0.80	+ 17	-01	+10	+08	+06	3.8	4.9	+126	+97	+ 20	+126	+96	+142 111	- 27 5	5 7	
3	3.50	- 72	-10	-07	-13	+08	2.5	5.7	-153	+63	- 67	-157	+89	-144 86	+ 59 7	7 7	
4	4.53	- 11	+04	+02	+05	-04	1.2	7.0	+ 27	- 22	- 13	+ 36	- 22	+ 41 24	+ 6 6	6 7	
5	5.43	- 15	+00	-02	-03	-02	0.8	7.4	- 6	- 7	- 13	- 7	- 9	+ 7 26	+ 5 8	8 7	
11	5.85	+ 3	-03	+14	+10	+10	2.8	5.5	+134	+134	- 7	+134	+134	+149 93	+ 15 11	1 7	
12	5.97	- 11	+06	+06	+09	-04	0.4	7.8	+ 19	- 9	- 13	+ 17	- 8	+ 33 12	+ 4 8	8 7	
13	6.01	+ 9	+02	-01	+01	-03	1.3	7.0	+ 4	- 18	+ 8	+ 4	- 18	+ 20 17	- 14 5	5 2	
20	6.12	- 14	-16	-01	-12	+18	1.4	6.8	- 76	+120	- 3	- 76	+120	- 61 47	- 4 9	9 7	
21	6.13	+ 3	+04	-04	-01	-07	1.6	6.6	- 5	- 53	+ 2	- 5	- 53	+ 10 22	- 7 8	8 3	
22	6.99	- 2	-06	-12	-14	+01	2.8	5.5	-187	+ 12	+ 21	-186	+ 12	-169 85	- 29 12	8 6	
23	7.00	+ 4	+09	+01	+07	-11	2.8	5.5	+ 94	-138	- 8	+ 94	-138	+100 41	+ 18 9	9 3	
24	7.05	+ 5	+03	-08	-05	-08	1.1	7.1	- 25	- 43	+ 9	- 24	- 43	- 9 17	- 15 8	8 3	
25	7.15	- 5	+10	+05	+12	-10	1.9	6.3	+104	- 88	- 17	+103	- 88	+117 64	+ 19 9	9 7	
26	7.15	- 17	+12	+46	+48	+08	1.1	7.1	+261	+44	- 48	+247	+43	+261 50	+ 47 10	7 7	
27	7.16	- 13	+04	-08	-04	-09	1.7	6.5	- 28	- 75	- 9	- 34	- 75	- 19 25	+ 5 6	6 3	
28	7.24	- 5	+09	+05	+11	-09	0.4	7.8	+ 21	- 17	- 8	+ 20	- 17	+ 35 14	- 1 1	8 7	
29	7.35	- 9	+12	+05	+13	-12	1.7	6.6	+101	- 96	- 22	+ 98	- 96	+113 49	+ 22 10	10 6.7	
30	7.35	- 23	+14	-30	-16	-32	1.8	6.4	-140	-376	- 7	-142	-376	-127 55	0 11	6.7	
31	7.48	- 19	+03	+41	+38	+16	0.8	7.4	+136	+59	- 37	+132	+59	+147 21	+ 31 9	9 7	
32	7.50	- 9	+06	+04	+08	-06	1.5	6.7	+ 56	- 40	- 17	+ 54	- 40	+ 60 50	+ 14 10	10 7	
36	7.69	- 14	+00	+15	+13	-07	2.1	6.1	+131	+71	- 32	+128	+71	+141 62	+ 38 11	11 6.7	
39	7.72	- 16	-21	-05	-26	+35	0.5	7.7	- 60	+ 83	- 6	- 61	+ 83	- 46 18	- 3 8	8 7	
42	7.93	- 7	-06	+39	+20	+26	0.7	7.5	+ 98	+ 86	- 19	+ 97	+ 86	+111 26	+ 13 9	9 7	
44	8.32	+ 5	-02	+13	+10	+08	0.5	7.7	+ 25	+ 21	+ 2	+ 26	+ 21	+ 41 18	- 10 8	8 7	
45	8.23	+ 6	-27	+08	-18	+37	2.1	6.1	-129	+361	- 18	-132	+360	-118 71	+ 12 13	13 7	
46	8.31	- 12	+10	+21	+25	-02	0.5	7.7	+ 55	- 5	- 20	+ 53	- 5	+ 67 17	+ 12 13	13 7	
48	8.47	- 24	+18	+22	+23	-11	0.5	7.7	+ 68	- 25	- 34	+ 64	- 24	+ 79 18	+ 26 8	8 7	
50	8.51	- 17	+03	+05	+06	-02	0.9	7.3	+ 28	- 7	- 21	+ 25	- 6	+ 40 30	+ 15 9	9 7	
52	8.53	+ 7	+04	+13	+01	-01	3.3	4.9	+205	+ 9	- 25	+204	+ 10	+215 112	+ 57 19	19 7	
54	8.81	- 20	+14	-07	-04	+20	0.9	7.8	- 16	+ 84	- 26	- 20	+ 81	- 6 39	+ 19 9	9 7	
55	8.93	- 6	+00	-02	-02	-01	1.9	6.8	- 14	- 13	- 4	- 15	- 13	0 37	+ 3 9	9 3	
57	9.02	- 6	-01	-03	-03	-01	0.8	7.5	- 11	- 8	- 4	- 12	- 3	+ 3 21	- 3 8	8 6.7	
58	10.05	- 4	-06	-16	-18	-01	1.6	6.6	-135	- 7	+ 19	-133	- 7	-117 55	- 26 13	13 7	
59	10.08	- 11	-04	-26	-34	-13	1.7	6.5	-279	-110	+ 39	-276	-110	-259 68	- 53 14	14 7.7	
60	10.36	- 27	+03	+03	+05	-03	1.8	6.4	+ 43	- 23	- 34	+ 28	- 24	+ 51 26	+ 37 9	9 2	
61	10.36	+ 3	+14	-14	-03	-24	2.4	5.9	- 29	-378	+ 4	- 29	-278	- 13 75	+ 1 16	7 7	
63	10.45	- 6	+05	+01	+04	-06	1.7	6.6	+ 24	- 49	- 14	+ 82	- 48	+ 47 24	+ 15 7	7 2	
67	10.75	- 5	+03	-02	+00	-05	1.6	6.6	+ 3	- 39	- 6	+ 2	- 39	+ 17 23	+ 6 6	6 3	
68	11.03	- 16	+21	-19	-03	-35	0.7	7.5	- 11	-121	- 23	- 16	-120	- 1 24	+ 15 9	9 7	
69	11.06	- 8	+20	-13	+02	-32	2.5	5.8	+ 29	-375	- 19	+ 26	-375	+ 39 83	+ 30 18	18 7	
71	11.26	+ 3	+06	-05	-00	-10	2.6	5.6	- 1	-130	+ 2	- 1	-130	+ 14 37	+ 8 11	11 3	
72	11.31	- 23	-01	+09	+07	+05	1.4	6.9	+ 48	+ 23	- 22	+ 43	+ 23	+ 57 45	+ 22 12	12 7	
73	11.40	+ 3	+22	+17	+20	-20	0.7	7.6	+ 90	- 63	- 23	+ 57	- 63	+103 25	+ 16 9	9 7	
74	11.41	- 9	-26	+05	-12	+34	1.1	7.1	- 66	+185	+ 25	- 63	+184	- 47 38	- 30 11	11 7	
75	11.65	- 8	+08	+06	+11	-08	0.8	7.6	+ 29	- 21	- 14	+ 27	- 21	+ 42 9	+ 7 8	8 2	
77	11.82	+ 6	+12	-04	+05	-17	0.3	8.0	+ 6	- 21	+ 5	+ 8	- 21	+ 23 7	- 14 8	8 6.7	
78	11.83	+ 17	-12	-48	-50	-08	2.9	5.4	-688	-114	+182	-671	-115	-636 123	-210 28	28 7	
79	11.83	- 13	-05	+09	+10	+01	2.1	6.3	+ 46	+ 99	- 21	+ 42	+ 99	+ 56 68	+ 29 16	16 7	
81	11.86	- 10	+25	-03	+15	-33	0.8	7.6	+ 53	-119	- 22	+ 49	-119	+ 64 36	+ 18 10	10 7	
83	11.97	+ 2	+17	-05	-06	-08	0.3	7.9	+ 12	-36	+ 1	+ 13	-36	+ 28 11	- 9 8	8 7	
83	11.98	0	-15	-06	-15	+15	2.8	5.5	-200	+198	+ 45	-195	+198	-175 93	+ 51 21	21 7	
85	12.00	- 8	+07	+07	+11	-06	0.9	7.4	+ 45	- 25	- 18	+ 42	- 24	+ 57 29	+ 14 10	10 7	
86	12.13	- 23	-09	-01	-07	+10	1.2	7.0	- 39	+ 58	- 15	- 48	+ 57	- 29 30	+ 11 13	13 7	
87	12.27	- 11	+10	-03	+04	-15	0.6	7.6	+ 13	- 43	- 14	+ 10	- 43	+ 25 21	+ 8 9	9 7	
89	12.57	- 3	+01	+19	+17	-07	2.5	5.8	+ 98	+ 87	- 47	+ 203	+ 87	+ 213 86	+ 78 21	21 7	
92	12.70	+ 9	+04	-03	+00	-07	1.2	7.0	+ 1	- 40	+ 8	+ 3	- 40	+ 19 17	+ 9 6	6 3	
93	12.71	- 1	+08	+02	+02	-06	2.2	6.1	- 40	- 62	+ 22	- 23	- 63	- 15 61	- 27 15	15 6.7	
95	13.09	+ 6	+04	-33	-26	-21	2.3	6.0	-284	-226	+ 84	-271	-225	-245 83	- 98 21	21 7	
96	13.16	- 23	-01	-11	-04	-04	0.8	7.9	- 14	- 6	- 19	- 19	- 3	- 4 9	+ 11 8	8 7	
99	13.36	- 17	+19	-06	+08	-27	1.5	6.7	+ 60	-197	- 27	+ 55	-197	+ 69 50	+ 81 14	14 7	
100	13.44	- 2	-02	-00	-01	+03	1.5	6.7	- 8	+ 13	- 0	- 8	+ 13	+ 7 49	+ 1 14	14 6	
101	13.44	- 26	+18	-23	-11	-28	0.5	7.7	- 28	- 73	- 18	- 24	- 73	- 19 18	+ 11 9	9 7	
102	13.46	- 16	+04	+15	+15	+03	0.3	7.9	+ 20	+ 4	- 20	+ 16	+ 3	+ 31 9	+ 12 8	8 7	
103	13.47	- 23	-08	+06	+00	+12	2.1	6.2	- 1	- 12	- 24	- 7	+ 121	+ 6 67	+ 22 17	17 7	
104	13.53	+ 6	+21	+02	+17	-26	2.1	6.3	+ 165	-258	- 28	+ 163	-258	+175 71	+ 48 19	19 7	
105	13.57	- 11	+15	-23	-10	-30	0.6	7.6	- 31	- 91	- 7	- 23	- 90	- 18 21	+ 1 9	9 7	
106	13.68	- 6	+02	-14	-11	-10	0.5	7.7	- 27	- 25	0	- 28	- 24	- 13 17	- 7 9	9 7	
107	13.69	- 8	+26	-00	-18	-33	3.0	5.8	-254	-477	- 80	+ 242	-477	+ 244 83	- 98 26	26 7	
113	13.91	- 31	+06	-15	-09	-14	0.7	7.6	- 28	- 45	- 20	- 24	- 47	- 19 33	+ 14 9	9 7	
115	13.95	- 18	-03	-09	-10	-00	1.0	7.2	- 49	- 1	- 6	- 52	- 1	- 27 33	+ 1 11	11 7	
116	13.96	- 5	-06	-31	-33	-04	2.6	5.7	-413	-55	+ 96	-402	-55	-374 101	- 126 26	26 7	
118	14.07	- 5	+10	+12	+17	-08	1.8	6.5	+ 151	- 66	- 43	+ 145	- 65	+ 157 62	+ 55 17	17 7	
119	14.14	- 18	+05	+17	+18	+01	0.6	7.6	+ 50	+ 3	- 29	+ 45	+ 3	+ 58 30	+ 24 9	9 7	
120	14.20	- 23	+33	-15	-09	-49	0.9	7.4	+ 39	- 204	- 25	+ 21	- 204	+ 46 29	+ 22 11	11 7	
121	14.23	- 4	-16	-05	-15	+17	0.8	7.4	- 60	+ 67	+ 12	- 59	+ 67	- 43 33	- 18 10	10 7	
122	14.25	- 7	+17	-34	-18	-38	2.3	5.1	-286	-601	+ 50	- 282	- 601	-257 113	- 6		

TABLE IV (*continued*)

Star No.	ℓ^{11}	ρ km/sec	μ_{α} 0°0000	μ_s 0°000	μ_i 0°000	μ_b 0°000	r kpc	R kpc	T_b km/sec	\dot{x} km/sec	\dot{y} km/sec	\dot{z} km/sec	$\Theta - \Theta_0$ km/sec	H km/sec	Source $\mu_{\alpha, \delta}$ (17)	
(1)	(2)	(3)	(4)	(5)	(6)	(7)	(8)	(9)	(10)	(11)	(12)	(13)	(14)	(15)	(16)	(17)
137	15°39	- 6	+04	+13	+14	+02	2.6	5.7	+171	+ 20	- 51	+163	+ 20	+170 ± 43	+ 88 ± 14	2
138	15.48	+ 14	+07	+03	+07	-07	1.9	6.4	+61	- 63	- 6	+62	- 64	+ 76	61	18
139	15.50	- 33	+22	+04	+18	-26	0.4	7.8	+33	- 46	- 41	+23	- 46	+ 37	13	33
141	15.57	- 19	+07	-07	-02	-12	1.3	6.9	- 10	- 74	- 13	- 13	- 75	+ 1	42	13
143	15.87	- 5	-01	-05	-06	-01	3.3	5.1	- 90	- 9	+ 19	- 88	- 9	- 70	106	4
145	16.03	+ 21	-31	-19	-39	+31	2.2	6.1	-400	+320	+131	-378	+320	-349	88	-156
147	16.20	- 17	-00	+15	+13	+07	2.1	6.2	+125	+ 74	- 49	+116	+ 75	+126	69	+ 71
148	16.21	- 16	-00	-15	-14	-07	2.0	6.3	-129	- 63	+ 21	-129	- 63	-111	66	- 22
149	16.42	- 22	+06	-18	-11	-16	0.8	7.4	- 42	- 61	+ 1	- 44	- 64	- 28	26	6
150	16.60	- 12	-01	-33	-30	-14	0.3	8.0	- 35	- 17	- 3	- 38	- 15	- 23	6	8
152	16.80	- 4	-01	+03	+01	+03	2.3	6.0	+ 16	+ 34	- 9	+ 14	+ 34	+ 28	73	+ 25
154	16.82	- 15	-06	+55	+44	+33	1.9	6.4	+400	+300	-138	+377	+299	+378	80	+179
155	16.85	+ 27	+07	-26	-19	-21	2.2	6.1	-197	-214	+ 72	-184	-216	-161	74	- 77
156	16.92	- 16	-07	-19	-22	+00	1.6	6.7	-186	+ 3	+ 33	-163	+ 3	-145	55	- 39
157	16.94	+ 27	+19	-19	-04	-33	2.6	5.7	- 49	-411	+ 46	- 37	-411	- 16	84	- 30
158	16.94	+ 25	+08	+05	+10	-07	2.2	6.1	+ 99	- 77	- 4	+ 102	- 77	+ 116	71	+ 28
160	16.96	+ 26	+19	-04	+09	-26	2.9	5.5	+126	-353	- 7	+130	-353	+141	93	+ 52
161	17.15	+ 3	-12	-03	-11	+14	1.0	7.2	- 56	+ 71	+ 24	- 52	+ 71	- 35	34	- 27
162	17.21	+ 9	+19	+23	+33	-13	1.6	6.7	+245	- 99	- 67	+236	- 99	+246	60	+ 89
164	17.54	- 25	+12	+08	+15	-11	0.7	7.5	+ 48	- 37	- 39	+ 38	- 37	+ 53	12	+ 36
165	17.66	- 36	-25	+08	-11	+36	2.1	6.2	-108	+360	- 14	-118	-358	-104	68	+ 15
166	17.66	- 7	+07	+14	+17	-02	1.7	6.6	+137	- 17	- 48	+129	- 16	+139	58	+ 66
167	17.69	- 4	+02	-11	-09	-07	2.1	6.2	- 86	- 74	+ 25	- 82	- 74	- 64	67	- 20
168	17.76	+ 5	+01	+02	+03	+00	1.6	6.7	+ 19	+ 3	- 1	+ 20	+ 3	+ 35	43	+ 8
170	17.98	- 13	+17	+09	+19	-17	1.9	6.4	+172	-156	- 68	+159	- 156	+167	64	+ 92
173	18.25	+ 1	+02	+06	+06	+01	1.4	6.9	- 39	+ 198	+ 21	- 34	+ 198	- 17	44	- 19
174	18.32	+ 23	+13	+15	+22	-09	2.6	5.8	+273	-115	- 61	+267	-115	+270	90	+121
176	18.44	- 8	-06	+09	+09	+12	1.6	6.7	+ 25	+ 93	- 18	+ 20	+ 92	+ 34	+ 26	18
178	18.48	+ 19	+22	-11	+05	-33	2.2	6.2	+ 48	-344	- 7	+ 48	-344	+ 62	69	+ 28
179	18.48	+ 2	+17	+19	+28	-13	1.7	6.6	+228	-105	- 75	+216	-105	+224	62	+101
180	18.62	- 6	-20	+09	-06	+30	1.4	6.9	- 39	+ 198	+ 21	- 34	+ 198	- 17	44	
181	18.79	- 9	+06	+09	+12	-03	2.6	5.8	+144	- 40	- 55	+133	- 40	+137	85	+ 97
182	18.91	- 11	+10	+01	+08	-12	1.7	6.6	+ 63	-100	- 25	+ 58	-100	+ 71	55	+ 39
183	18.99	- 14	+29	-32	-09	-52	1.6	6.7	- 68	-392	+ 1	- 71	-391	- 56	51	+ 1
184	19.39	- 46	+05	-01	+03	-06	2.2	6.2	+ 27	- 64	- 57	+ 8	- 60	+ 16	69	+ 74
185	20.02	+ 32	+07	+30	+31	+05	1.9	6.4	+278	+ 48	- 65	+272	+ 48	+279	69	+ 106
186	20.04	+ 54	-03	-02	-04	+03	3.0	5.5	- 63	+ 46	+ 74	- 40	+ 44	- 13	95	- 47
187	21.03	- 11	+03	+09	+09	+00	1.2	7.1	+ 54	+ 2	- 29	+ 46	+ 3	+ 59	38	+ 36
188	21.06	- 17	+05	-16	-11	-14	0.2	8.0	- 10	- 12	- 15	- 12	0	3	+ 4	5
189	21.43	- 16	+09	+27	+30	+01	1.0	7.2	+150	+ 6	- 69	+134	+ 7	+146	38	+ 78
192	21.91	- 28	+09	-06	+01	-14	1.7	6.6	+ 4	-119	- 25	- 5	- 119	+ 7	54	+ 37
193	22.16	- 14	+26	-00	+17	-34	1.8	6.6	+147	-292	- 80	+126	-291	+132	59	+ 107
196	23.97	+ 50	-08	-23	-26	-00	0.7	7.6	- 87	0	+ 81	- 59	- 2	- 41	24	- 85
197	24.02	+ 4	+11	-09	-01	-18	0.7	7.6	- 2	- 57	0	- 2	- 57	+ 13	20	- 2
201	25.05	+ 23	-02	+12	+09	+08	2.1	6.4	+ 86	+ 81	- 15	+ 88	+ 81	+100	64	+ 48
203	25.20	- 11	-05	-08	-11	+03	2.1	6.4	-110	+ 29	+ 37	-104	+ 29	-83	64	- 29
204	25.32	- 46	-13	-06	-14	+15	1.9	6.5	+126	+134	+ 18	-131	-136	-113	59	- 16
206	25.46	- 16	+05	-12	-08	-12	0.4	7.8	- 15	- 24	- 7	- 20	- 25	- 5	13	+ 9
207	25.78	- 50	-04	-12	-14	+00	2.1	6.4	+134	+ 3	+ 14	-142	+ 11	-124	65	- 12
208	25.81	+ 6	+09	+06	+12	-09	1.0	7.3	+ 56	- 41	- 20	+ 52	- 41	+ 66	31	+ 26
210	25.94	- 7	-05	-06	-08	+05	1.8	6.6	- 66	+ 41	+ 25	- 61	+ 41	- 43	55	- 15
212	28.16	- 4	-02	-03	-04	+02	2.5	6.1	- 44	+ 19	+ 17	- 40	+ 19	- 24	74	+ 9
213	28.24	- 15	+11	-10	-02	-19	0.2	8.0	- 2	- 19	- 15	- 10	- 16	+ 5	4	+ 2
214	28.55	- 7	+09	+07	+13	-09	0.6	7.7	+ 37	- 25	- 26	+ 28	- 25	+ 43	19	+ 26
215	29.06	- 14	-02	-25	-24	-08	0.3	8.0	- 30	- 10	+ 1	- 34	- 8	- 19	5	- 9
222	32.58	- 6	-13	-07	-15	+14	1.1	7.3	- 82	+ 77	+ 43	- 69	+ 77	- 50	34	- 40
223	33.06	- 4	-01	-07	-02	0.4	7.8	- 14	- 4	+ 4	+ 4	- 14	- 4	+ 2	13	- 8
224	33.85	+ 7	-01	-08	-08	-02	0.7	7.6	- 25	- 8	+ 19	- 17	- 8	- 1	20	- 19
225	34.13	- 22	+03	-07	-04	-08	0.4	7.9	- 8	- 13	- 13	- 18	- 16	- 3	5	+ 8
226	34.39	- 9	-09	-08	-13	+08	0.7	7.6	- 44	+ 26	+ 14	- 44	+ 24	- 28	10	- 15
227	34.74	- 10	-02	-11	-11	-03	0.3	7.9	- 17	- 4	+ 2	- 19	- 5	- 4	10	- 8
228	37.51	+ 29	-11	-04	-11	+13	2.9	6.2	+149	+172	+117	- 97	+171	- 51	78	- 85
229	37.81	+ 23	+00	-03	-02	-02	3.3	5.9	- 37	- 25	+ 40	- 16	- 26	+ 4	87	+ 25
230	40.62	+ 6	-12	+19	+09	+24	0.7	7.7	+ 30	+ 76	- 19	+ 23	+ 76	+ 37	18	+ 22
241	41.14	- 9	+00	+01	+01	+00	1.4	7.2	+ 6	+ 1	- 11	- 1	+ 2	+ 12	15	+ 29
244	41.71	- 84	+05	+04	+08	-05	1.7	7.0	+ 59	- 41	- 100	- 10	- 45	- 12	42	+ 123
245	42.85	- 23	+07	+00	+06	-10	0.3	8.0	+ 8	- 14	- 21	- 9	- 15	+ 5	5	+ 3
246	43.07	- 10	-03	+10	+07	+08	0.2	8.0	+ 7	+ 8	- 12	- 2	- 8	+ 13	4	+ 6
247	43.26	- 5	+02	-03	-01	-05	0.2	8.1	- 1	- 3	- 3	- 4	- 3	+ 11	4	- 4
248	44.33	- 9	+09	-06	+01	-15	0.5	7.8	+ 3	- 38	- 9	- 4	- 37	+ 10	14	+ 9
249	44.64	- 27	-09	+09	+01	+16	0.6	7.8	+ 4	+ 43	- 17	- 11	- 46	+ 3	14	+ 17
250	45.57	- 9	-15	+00	+10	-19	0.7	7.7	- 33	+ 62	+ 18	- 29	+ 62	- 12	17	- 15
251	45.81	- 10	+02	+09	+09	+01	1.5	7.2	+ 67	+ 9	- 54	+ 41	+ 10	+ 46	17	+ 84
254	46.83	- 28	-01	-00	-01	+01	0.8	7.7	- 3	- 3	- 16	- 22	- 7	- 8	9	+ 22
255	47.02	- 7	+03	-01	+01	-04	0.4	7.9	+ 2	- 7	- 6	- 3	- 8	+ 12	5	+ 4
257	47.36	- 33	+11	-13	-04	-20	0.4	7.9	- 8	- 37	- 16	- 29	- 37	- 15	10	+ 13
258	48.71	+ 1	-02	-17	-11	-16	0.3	8.0	+ 11	+ 11	- 7	+ 9	+ 11	+ 24	8	+ 5
260	49.23	- 13	-03	+14	+10	+10	0.2	8.0	+ 11	+ 12	- 16	- 1	+ 13	+ 14	7	+ 10
261	49.74	+ 4	+08	-05	+01	-12	0.2	8.0	+ 1	- 14	+ 2	+ 3	- 14	+ 19	4	- 7
262	50.07	- 17	+01	-17	-15	-09	2.3	7.0	-158	- 97	+110	-114	- 97	- 73	51	- 88
263	50.91	- 14	-01	-17	-16	-07	0.2	8.1</								

TABLE IV (*continued*)

Star No. (1)	ℓ^{II} (2)	ρ km/sec (3)	μ_α 0.0000 (4)	μ_δ 0.0000 (5)	μ_i 0.0000 (6)	μ_b 0.0000 (7)	r kpc (8)	R kpc (9)	T_1 km/sec (10)	T_2 km/sec (11)	\dot{x} km/sec (12)	\dot{y} km/sec (13)	\dot{z} km/sec (14)	$\Theta - \Theta_0$ km/sec (15)	Π km/sec (16)	Source μ_{α}, δ (17)
724	170.04	0	-11	-04	-05	-13	1.4	9.6	-32	-86	+ 5	+ 32	- 86	+ 47 ± 20	- 9 ± 6	2
726	170.23	+	5	+14	-12	+18	+08	0.3	8.5	+ 23	+ 11	- 6	- 22	+ 11	- 7	8
729	172.09	+	59	-05	+25	-33	+15	0.6	8.8	- 97	+ 46	- 47	+ 105	+ 44	+ 119	16
730	172.77	-	29	+06	-14	+16	-02	1.6	9.8	+119	- 17	+ 14	- 122	- 17	- 106	28
739	174.55	+	11	+10	-15	+19	+02	1.3	9.5	+116	+ 11	- 22	- 115	+ 11	- 100	39
745	175.78	0	-00	-02	+02	-01	1.0	9.2	+ 9	- 7	0	- 9	- 7	+ 6	14	2
746	177.17	+	17	-07	+01	-07	-07	0.2	8.4	- 7	- 7	- 15	+ 8	- 10	+ 23	4
748	179.04	+	30	-01	-04	+03	-03	0.3	8.5	+ 4	- 5	- 30	- 3	- 5	+ 12	4
750	179.26	+	16	+01	-04	+04	-01	0.2	8.4	+ 5	- 1	- 16	- 4	- 4	+ 11	3
751	179.62	+	4	-05	-00	-03	-06	0.3	8.5	- 4	- 7	+ 4	- 7	- 7	+ 19	5
752	179.90	+	1	-02	-10	+07	-08	0.2	8.4	+ 7	- 8	0	- 7	- 8	+ 8	3
753	180.10	+	20	-11	-17	+07	-22	0.3	8.5	+ 8	- 26	+ 18	- 8	- 27	+ 7	6
754	181.90	+	15	+10	-23	+27	-01	0.3	8.5	+ 34	- 1	+ 14	- 34	- 2	- 19	5
755	182.27	+	18	-15	-17	+05	-25	2.5	10.7	+ 61	- 303	+ 36	- 63	- 301	- 48	48
756	182.76	+	19	-10	+02	-09	-10	0.8	9.0	- 31	- 37	- 19	+ 30	- 38	+ 46	12
757	182.96	+	23	+06	-15	+18	-01	0.2	8.4	+ 16	- 1	- 22	- 17	- 3	- 2	3
759	183.75	+	14	+02	-10	+11	-03	0.2	8.4	+ 9	- 3	- 13	- 10	- 4	+ 5	3
760	183.97	+	8	-01	-00	-01	-01	1.3	9.5	- 3	- 7	- 8	+ 3	- 6	+ 18	19
762	184.59	+	12	-04	-01	-02	-05	1.0	9.2	- 7	- 23	- 9	- 7	- 24	+ 22	14
763	184.62	+	19	+03	-19	+19	-06	0.5	8.7	+ 41	- 14	- 15	- 42	- 15	- 27	9
764	185.69	+	24	+02	-22	+21	-09	0.2	8.4	+ 18	- 8	- 22	- 20	- 10	- 5	4
765	186.57	+	15	-02	-05	+03	-05	2.1	10.3	+ 31	- 46	- 11	- 33	- 46	- 18	40
766	186.58	+	11	-01	-08	+06	-05	0.8	9.0	+ 24	- 19	- 8	- 25	- 19	- 10	15
767	186.62	+	14	+01	-09	+09	-03	1.7	9.9	+ 68	- 24	- 6	- 69	- 24	- 54	33
768	187.06	+	19	+03	-23	+23	-09	0.1	8.3	+ 16	- 6	- 16	- 18	- 9	- 3	3
769	187.40	+	44	-01	-03	+02	-02	0.3	8.5	+ 3	- 3	- 42	- 9	- 9	+ 6	4
771	187.76	+	16	+05	-05	+08	+04	1.3	9.5	+ 49	+ 25	- 8	- 50	+ 25	- 36	20
772	187.99	+	13	+06	-05	+08	+05	1.4	9.6	+ 57	+ 36	- 3	- 58	+ 36	- 43	22
773	188.01	+	31	-01	-05	+03	-05	0.3	8.5	+ 5	- 7	- 29	- 9	- 12	+ 6	4
774	188.50	+	18	-02	-06	+04	-05	1.5	9.7	+ 28	- 35	- 16	- 31	- 18	- 22	+ 1
775	188.60	+	16	-01	+02	-02	+00	1.0	9.1	- 10	+ 1	- 17	+ 8	+ 1	+ 23	14
776	188.97	+	7	-01	-11	+09	-06	0.4	8.6	+ 17	- 12	- 4	- 17	- 2	- 2	6
777	189.10	+	9	+02	-02	+03	+02	1.5	9.7	+ 22	+ 14	- 5	- 23	+ 14	- 8	29
778	189.69	+	17	+06	-09	+08	-04	1.3	9.5	+ 50	- 25	- 8	- 52	- 25	- 38	20
780	190.09	+	21	+04	-21	+21	-07	0.3	8.4	+ 25	- 8	- 15	- 28	- 11	- 13	5
782	190.81	-	7	-03	+07	-08	+00	2.1	10.3	- 80	+ 2	- 8	+ 80	+ 2	+ 94	40
783	191.09	+	19	-03	-06	+03	-08	0.2	8.4	+ 3	- 8	- 16	- 6	- 11	+ 9	3
785	192.16	+	32	+05	+01	+02	+06	0.3	8.5	+ 4	+ 10	- 31	- 11	+ 7	+ 4	5
786	192.16	+	17	+01	-15	+14	-05	0.8	9.0	+ 55	- 21	- 6	- 57	- 20	- 43	28
787	192.40	+	10	+08	-11	+15	+05	3.0	11.2	+ 215	+ 78	+ 41	- 211	+ 78	- 199	102
788	192.42	+	39	-04	-17	+12	-12	0.1	8.3	+ 5	- 5	- 38	- 14	- 2	+ 1	2
789	192.84	-	5	-04	-22	+16	-16	0.4	8.6	+ 30	- 31	- 13	- 28	- 31	- 13	4
790	193.18	+	28	+06	-14	+17	-00	0.3	8.5	+ 24	0	- 22	- 29	- 4	- 14	5
791	194.07	-	18	-08	+02	-08	-10	3.2	11.3	- 117	- 144	+ 3	+ 122	- 142	+ 135	103
792	194.13	+	22	+04	-17	+17	-04	0.1	8.3	+ 12	- 3	- 18	- 17	- 3	- 2	3
793	194.14	-	18	-05	-05	+00	-09	2.3	10.4	+ 5	- 5	- 38	- 14	- 2	+ 1	2
795	194.80	+	22	+06	-21	+22	-04	0.2	8.4	+ 16	- 3	- 17	- 21	- 4	- 6	3
797	195.58	-	1	-01	-07	+05	-05	1.1	9.3	+ 26	- 27	+ 9	- 25	- 27	- 10	30
798	195.62	+	15	+06	-22	+25	-01	1.1	9.3	+ 128	- 5	+ 20	- 127	- 6	- 113	35
801	195.65	+	32	-06	+10	-13	-03	1.1	9.3	- 69	- 17	- 49	+ 58	- 18	+ 74	36
804	195.81	+	24	+01	-20	+18	-09	0.1	8.3	+ 12	- 6	- 20	- 18	- 7	- 3	3
806	196.16	+	14	+15	+01	+09	+19	0.9	9.0	+ 39	+ 79	- 6	- 42	+ 78	- 27	24
807	196.34	+	20	-01	-15	+12	-10	1.1	9.3	+ 62	- 46	- 2	- 66	- 45	- 51	36
808	196.42	+	30	-00	-12	+10	-06	0.3	8.5	+ 15	- 9	+ 33	- 6	- 9	+ 9	9
809	196.49	+	36	+18	+04	+09	+24	0.8	8.9	+ 31	+ 88	- 28	- 41	+ 87	- 25	11
810	196.96	+	10	+07	+00	+04	+09	1.0	9.2	+ 21	+ 43	- 2	- 22	+ 43	- 8	29
811	197.55	+	8	-03	-04	-02	-05	0.8	9.0	+ 9	- 20	- 8	- 12	- 19	+ 3	11
814	199.00	+	19	-03	-01	-02	-05	0.3	8.4	- 2	- 6	- 18	- 4	- 6	+ 6	5
816	199.25	+	7	-03	-08	+05	-08	0.4	8.6	+ 8	- 14	- 2	- 10	- 15	+ 5	3
817	199.56	+	27	-00	-02	+01	-01	1.4	9.6	+ 9	- 8	- 22	- 17	- 8	- 2	45
819	200.63	-	20	+04	-02	+04	+04	0.7	8.9	+ 14	+ 14	+ 24	- 6	+ 14	+ 8	10
820	200.85	+	41	-03	+15	+18	+08	1.0	9.1	+ 74	+ 15	+ 15	- 68	+ 54	+ 71	33
821	201.82	+	23	+04	-20	+20	-04	0.6	8.7	+ 55	- 12	- 0	- 59	- 14	- 45	11
823	202.04	+	16	-07	-06	-00	-12	1.0	9.2	- 0	- 60	- 16	- 6	- 60	+ 9	32
825	202.93	+	33	+01	-04	-01	1.0	9.1	+ 16	- 3	- 24	- 28	- 2	- 13	13	7
826	202.95	+	18	+01	-20	+18	-08	0.8	8.9	+ 64	- 29	+ 7	- 66	- 28	- 52	25
828	203.03	+	23	+05	+05	-01	+08	1.7	9.9	+ 3	- 29	- 21	- 6	- 29	+ 26	23
829	203.13	+	6	+03	+06	-04	+07	0.8	8.9	- 14	+ 24	- 10	+ 11	+ 24	- 8	12
831	203.34	+	19	-00	-16	+14	-08	1.3	9.4	+ 91	- 49	+ 17	- 91	- 49	- 38	36
832	203.43	+	26	-05	-24	+17	-18	1.2	8.4	+ 20	- 21	- 14	- 28	- 23	- 13	7
833	203.49	+	38	-11	+12	-19	-09	1.8	9.9	- 161	- 77	- 99	+ 133	- 77	+ 153	52
840	204.72	+	10	-02	-07	+05	-06	0.3	8.5	+ 7	- 9	- 7	- 11	- 8	+ 4	4
842	204.89	+	34	+02	-20	+19	-07	0.3	8.5	+ 28	- 10	- 17	- 38	- 15	- 23	10
843	205.02	+	13	-04	-08	+04	-09	0.3	8.4	+ 5	- 11	- 9	- 9	- 12	+ 6	4
844	205.33	-	1	+07	-15	+18	+02	0.5	8.7	+ 46	+ 6	+ 21	- 41	+ 6	- 27	15
845	205.35	+	32	-02	+05	-06	-00	1.6	9.7	- 48	- 2	- 49	+ 29	- 2	+ 46	21
847	205.81	+	38	+07	+11	-05	+14	1.8	9.9	- 46	+ 124	- 55	+ 25	+ 124	+ 24	24
848	205.87	+	25	+01	+00	+01	1.1	9.2	+ 1	+ 7	- 22	- 12	+ 7	+ 4	14	
852	206.20	+	13	+02	-16	+15	-05	1.4	9.5	+ 99	- 31	+ 33	- 94	- 31	- 82	43
853	206.20	+	31	+04	+00	+06	1.7	9.7	+ 4	+ 49	- 26	- 16	+ 50	- 1	- 1	21
854	206.22	+	34	-01	-24	+20	-12	1.8	9.9	+ 174	- 107	+ 50	- 169	- 108	- 159	32
856	206.31	+	36	+06	-02	+06	-00	1.5	9.6	+ 40	+ 51	- 16	- 53	+ 49		

TABLE IV (continued)

Star No.	μ_1	ρ km/sec	μ_2 0°0'000	μ_3 0°0'000	μ_4 0°0'000	μ_5 0°0'000	r	R kpc	T_1 km/sec	T_2 km/sec	\dot{x} km/sec	\dot{y} km/sec	\dot{z} km/sec	$\Theta - \Theta_0$ km/sec	Π km/sec	Source $\Delta\alpha, \delta$	
(1)	(2)	(3)	(4)	(5)	(6)	(7)	(8)	(9)	(10)	(11)	(12)	(13)	(14)	(15)	(16)	(17)	
872	207.33	+ 20	-11	+07	-14	-11	1.6	9.6	-107	-84	-66	+ 87	-84	+106	+49	+ 31	±26
873	207.25	+ 18	-08	+13	-18	-04	1.7	9.7	-138	-85	-79	+114	-35	+134	52	+ 41	28
874	207.36	+ 6	-08	-03	-03	-12	1.0	9.1	-16	-56	-12	+ 12	-56	+26	30	- 11	17
877	208.07	+ 9	-12	-05	-04	-18	0.4	8.5	-7	-31	-8	+ 4	-32	+ 19	11	- 8	7
878	208.44	+ 10	+01	-02	+03	+00	0.8	8.9	+ 11	+ 1	-3	-14	+ 1	0	11	- 17	7
880	208.54	+ 35	-01	+01	-01	-01	1.1	9.2	-7	-6	-33	-11	-6	+ 5	15	+ 10	9
881	208.59	+ 18	+10	+07	+00	+17	1.2	9.3	+ 2	+ 95	-19	-12	+ 94	+ 3	35	- 5	30
882	208.73	+ 11	+07	-07	+11	+06	1.9	9.9	+ 97	+ 57	+ 35	-91	+ 56	- 81	57	- 58	32
883	208.74	+ 30	-17	-14	+00	-29	2.0	10.0	+ 2	-273	-14	-10	-274	+ 4	58	- 17	33
885	209.17	+ 34	-14	+03	-12	-17	0.4	8.6	-24	-35	-44	+ 3	-31	+ 19	6	+ 26	5
888	210.02	+ 58	-04	-05	+01	-07	1.3	9.3	+ 8	-44	-45	-35	-46	-18	31	+ 22	18
889	210.07	+ 9	+05	-10	+13	+02	1.1	9.2	+ 66	+ 10	+ 25	-62	+ 10	-49	28	- 46	17
890	210.29	+ 10	-03	-03	+00	-05	0.2	8.4	0	-5	-8	-5	-6	+ 10	6	- 5	5
892	210.41	+ 10	-09	-16	+08	-20	2.4	10.3	+ 96	-232	+ 44	-85	-223	-78	60	- 71	36
894	211.77	+ 23	-01	-00	-00	-01	0.8	8.9	-1	-5	-20	-11	-5	+ 4	10	- 1	7
895	211.85	- 1	-17	-19	+06	-31	2.1	10.0	+ 55	-312	+ 32	-45	-312	-36	59	- 62	37
896	211.99	+ 25	-03	-23	+18	-14	0.1	8.3	+ 12	-9	-14	-23	-11	-8	3	+ 2	4
898	212.62	+ 8	+04	+08	-05	+09	0.4	8.6	-9	+19	-14	+ 2	+ 17	+ 17	10	- 3	8
909	213.06	+ 7	-04	-09	+05	-09	0.4	8.5	+ 10	-17	-2	-13	-16	+ 2	10	- 13	6
900	213.10	+ 36	-09	+11	-16	-07	2.3	10.2	-170	-76	-124	+122	-75	+148	67	+ 69	44
904	214.03	+ 15	-02	-02	+00	-03	0.3	8.5	+ 1	-5	-11	-8	-6	+ 7	8	- 4	7
905	214.21	+ 10	+05	-08	+11	+04	0.2	8.4	+ 10	+ 3	-3	-14	+ 2	+ 1	4	- 10	4
906	214.52	+ 25	-03	+00	-02	-03	0.3	8.5	-3	-5	-21	-11	-8	+ 4	5	+ 6	5
911	215.83	+ 29	+02	+20	-17	+12	1.6	9.5	-126	+ 93	-103	+ 81	+ 90	+103	45	+ 62	33
913	216.36	+ 29	-02	+01	-03	0.3	8.5	+ 1	-5	-22	-17	-10	-2	5	+ 6	5	2
914	216.42	+ 25	-14	-11	+00	-24	1.7	9.6	+ 4	-185	-18	-18	-185	-4	45	- 14	33
916	216.66	+ 22	-03	-03	+01	-05	0.3	8.4	+ 1	-6	-16	-13	-9	+ 2	4	+ 2	5
917	216.66	+ 18	-11	+04	-11	-12	0.3	8.4	-13	-15	-21	+ 1	-17	+ 16	7	+ 6	6
920	216.87	+ 60	-03	+07	-08	-01	1.8	9.7	-68	-5	-88	+ 18	-6	+ 41	49	+ 50	57
923	217.33	+ 23	+05	-04	+08	+05	0.3	8.4	+ 10	+ 7	-12	-23	+ 5	- 8	5	- 2	5
925	217.52	+ 15	-03	-14	+10	-10	0.8	8.8	+ 39	-36	+ 16	-37	-38	-24	22	- 37	18
926	217.67	+ 13	-04	-01	-06	-13	1.3	9.3	-8	-35	-14	0	-35	+ 14	15	- 17	13
927	218.01	+ 25	-03	-00	-02	-04	0.4	8.5	-3	-7	-22	-13	-7	+ 2	5	+ 5	2
933	219.11	+ 22	-02	-19	+16	-10	0.8	8.8	+ 59	-39	+ 24	-56	-42	-44	22	- 44	18
934	219.13	+ 5	-04	-14	+10	-11	1.7	9.5	+ 79	-90	+ 47	-64	-90	-56	38	- 75	31
938	221.28	+ 24	-18	+03	-14	-22	1.1	9.1	-73	-114	-56	+ 48	-116	+ 65	29	+ 23	26
941	221.97	+ 7	+15	+18	-07	+27	0.3	8.4	-11	+ 41	-18	-1	+ 39	+ 14	9	+ 1	9
943	222.09	+ 25	-06	-10	+05	-13	0.8	8.8	+ 17	-46	-1	-23	-50	-9	16	- 22	15
944	222.18	+ 51	-04	-15	+11	-12	1.8	9.6	+ 96	-101	+ 29	-103	-94	40	- 56	36	6.7
945	222.31	+ 38	+00	-20	+18	-09	1.7	9.5	+143	-70	+ 69	-130	-70	-125	44	- 90	40
946	222.40	+ 42	-12	+06	-13	-13	2.6	10.3	-164	-156	-139	+ 94	-157	+127	67	+ 71	61
947	222.43	+ 2	-09	-09	+02	-16	0.5	8.6	+ 4	-37	+ 6	0	-38	+ 14	11	- 25	10
948	222.66	- 10	+01	+06	+05	+03	0.3	8.4	-7	+ 5	+ 2	+ 11	+ 6	+ 26	9	- 19	6
950	223.72	+ 19	-18	-35	+19	-39	0.9	8.9	+ 83	-170	+ 48	-69	-176	-59	21	- 70	20
951	224.05	+ 3	-21	-00	-14	-28	1.2	9.1	-79	-161	-45	+ 67	-160	+ 83	30	+ 7	29
952	224.05	+ 16	+06	-11	+14	+03	1.0	9.0	+ 71	+ 16	+ 38	-63	+ 16	- 52	23	- 61	23
953	224.17	+ 58	+04	+04	-00	+08	1.3	9.2	-2	+ 48	-44	-39	+ 47	- 22	14	+ 14	14
954	224.18	+ 16	-11	+15	-20	-07	0.7	8.7	-70	-24	-50	+ 40	-25	+ 57	17	+ 33	17
956	224.41	+ 23	+05	+17	-11	+15	1.2	9.1	-64	+ 86	-58	+ 32	+ 87	+ 51	14	+ 23	14
957	224.48	+ 14	+14	-05	+14	+16	0.3	8.5	+ 24	+ 27	+ 7	-27	+ 27	- 12	10	- 23	10
959	224.69	+ 18	+00	-06	+06	-02	0.3	8.5	+ 10	-4	-6	-19	-4	- 5	9	- 11	9
960	224.70	+ 6	+19	-01	+14	+24	0.8	8.8	+ 51	+ 89	+ 25	-47	+ 88	- 35	20	- 47	20
961	224.71	+ 31	-05	+01	-04	-06	0.6	8.6	-10	-15	-29	-14	-16	+ 2	7	+ 8	7
964	224.73	+ 33	-02	-05	+03	-04	1.3	9.2	+ 21	-28	-8	-38	-27	-24	14	- 22	14
967	225.44	+ 16	-14	+05	-14	-17	1.1	9.0	-71	-87	-55	+ 45	- 88	+ 63	27	+ 20	27
970	225.68	+ 33	-08	+02	-07	-10	1.7	9.4	-58	-80	-62	+ 19	-81	+ 39	18	+ 20	18
971	225.95	+ 19	+02	+06	-04	+05	1.0	9.0	-21	+ 23	-29	0	+ 22	+ 16	12	- 1	12
972	226.11	+ 30	-06	-16	+10	-15	0.3	8.4	+ 12	-18	-31	-31	-16	6	- 2	6	6.7
979	227.58	+ 17	+05	-11	+13	+01	0.3	8.4	+ 20	+ 1	+ 3	-26	-1	-11	9	- 20	9
982	228.33	- 1	-13	-21	+10	-27	1.7	9.4	+ 81	-211	+ 75	-38	-209	-36	38	-110	42
984	228.59	+ 24	+00	+15	-13	+08	1.5	9.3	-96	+ 59	-80	+ 53	+ 62	+ 75	35	+ 34	39
985	228.70	+ 41	-02	+06	-07	-00	0.5	8.5	-15	-1	-38	-21	-6	- 5	6	+ 19	6
986	228.99	+ 16	-05	-01	-03	-07	2.3	9.9	-28	-80	-29	+ 10	-81	+ 24	50	- 24	58
987	229.07	- 28	-03	-01	-05	0.4	8.5	-2	-9	+ 17	+ 23	-7	+ 37	10	- 36	11	7
988	229.13	+ 17	-03	-23	+18	-15	1.4	9.2	+119	-99	+ 81	-88	-99	-84	32	-107	37
991	229.42	+ 6	-03	-07	+04	-08	1.3	9.1	+ 25	-45	+ 16	-19	-45	- 8	12	- 49	14
993	229.74	+ 5	+06	+35	+25	+27	0.3	8.4	-32	+ 33	-27	+ 18	+ 33	+ 33	8	+ 10	8
994	229.85	+ 65	-17	+06	-17	-19	1.5	9.2	-123	-139	-134	+ 32	-140	+ 60	34	+ 89	41
996	230.46	+ 22	-09	+04	-10	-10	0.6	8.6	-31	-30	-38	+ 2	-29	+ 18	12	+ 15	15
997	230.91	+ 21	-01	-02	+01	-03	0.6	8.6	+ 2	-7	-12	-18	-6	- 3	6	- 9	7
998	231.08	- 5	+01	-21	+19	-09	0.5	8.5	+ 43	-21	+ 36	-23	-21	-11	7	- 56	8
1000	231.31	+ 31	-01	+06	-06	+01	0.6	8.6	-16	+ 3	-32	-14	-2	+ 2	7	+ 10	7
1001	231.35	+ 15	+11	-20	+25	+04	1.5	9.2	+ 178	+ 28	+ 130	-122	+ 28	-126	35	-153	44
1014	233.37	+ 15	-03	+06	-08	-01	1.1	8.9	-43	-6	-44	+ 13	-5	+ 30	24	+ 8	31
1016	233.73	+ 9	-07	-20	+14	-18	0.4	8.4	+ 24	-31	+ 17	-18	-32	- 4	8	- 34	9
1018	234.02	+ 38	-01	-06	+05	-04	0.6	8.6	+ 15	-12	-9	-38	-18	-23	7	- 13	8
1020	234.20	+ 16	+02	-11	+11	-03	2.4	9.8	+ 122	-36	+ 89	-84	-36	-92	48	-127	66
1022	234.83	+ 30	+09	+													

TABLE IV (*continued*)

Star No.	ρ	ρ	μ_α	μ_δ	μ_α	μ_δ	μ_α	μ_δ	τ	R	T_i	T_b	\dot{z}	\dot{i}	\dot{z}	$\Theta - \Theta_0$	Π	Π	Source
(1)	(2)	(3)	(4)	(5)	(6)	(7)	(8)	(9)	(10)	(11)	(12)	(13)	(14)	(15)	(16)	(17)	μ_α, δ		
1058	238.90	+	14	-05	-24	+17	-19	0.3	8.4	+ 28	- 32	+ 15	- 29	- 30	- 15 ± 8	- 32 ± 11	7		
1059	238.97	0	-06	-03	-01	-09	0.2	8.3	- 1	- 9	0	+ 1	- 9	+ 16	5	- 15	4	3	
1060	239.04	+	19	-07	-11	+04	-15	0.2	8.3	+ 3	- 11	- 8	- 19	- 9	- 4	4	- 6	3	2
1061	239.20	+	7	-03	+07	-09	-00	0.9	8.7	- 37	0	- 35	+ 13	0	+ 29	8	+ 3	12	3
1063	239.41	+	26	-04	+07	-09	-02	0.2	8.3	- 8	- 1	- 20	- 18	- 5	- 3	5	+ 5	4	3
1067	241.96	+	33	-20	+23	-33	-12	0.1	8.3	- 21	- 7	- 34	- 19	- 9	- 4	5	+ 20	5	6
1068	242.08	+	14	+00	+06	-05	+03	0.8	8.6	- 19	+ 10	- 24	- 5	+ 7	+ 10	11	- 4	19	6
1073	243.21	+	28	-01	-05	+04	-03	0.4	8.4	+ 9	- 7	- 4	- 28	- 11	- 13	5	- 16	6	3
1074	243.42	+	7	-13	+06	-13	-12	0.5	8.4	- 29	- 26	- 27	+ 9	- 26	+ 25	9	+ 5	13	6
1077	245.04	+	8	-10	-01	-05	-11	0.5	8.4	- 11	- 25	- 12	0	- 26	+ 15	7	- 10	12	6
1078	245.15	+	21	-06	+01	-04	-06	0.3	8.3	- 5	- 7	- 13	- 16	- 10	- 1	5	- 3	7	6
1082	248.78	+	19	-06	-03	-01	-08	0.3	8.3	- 1	- 11	- 7	- 15	- 14	0	5	- 10	8	6.5
1083	248.82	+	23	-05	+03	-06	-05	0.2	8.3	- 6	- 5	- 13	- 18	- 9	- 3	5	- 2	6	6.5
1084	248.88	+	36	+03	-08	+09	+00	0.8	8.5	+ 34	+ 1	+ 19	- 46	- 6	- 34	10	- 46	22	6.5
1086	249.46	+	21	-13	-01	-06	-14	0.6	8.4	- 18	- 38	- 22	- 8	- 40	+ 7	7	- 3	16	6.5
1087	249.85	-	10	-11	-01	-05	-12	0.3	8.3	- 9	- 19	- 4	+ 15	- 18	+ 29	6	- 16	9	6
1088	250.46	+	19	-07	-01	-03	-07	0.2	8.3	- 4	- 8	- 9	- 16	- 10	- 1	5	- 7	6	6
1089	250.52	-	54	-05	-01	-02	-06	0.3	8.3	- 4	- 10	+ 14	+ 52	- 11	+ 66	5	- 36	5	3
1090	251.48	+	28	+03	-03	+04	+02	0.2	8.3	+ 4	+ 2	+ 5	- 28	- 10	- 13	5	- 10	6	6.5
1091	251.55	+	23	+01	-11	+10	-04	0.4	8.3	+ 20	- 7	+ 12	- 27	- 10	- 13	5	- 31	6	3
1092	252.13	+	23	-10	+13	-18	-04	0.3	8.3	- 22	- 6	- 28	- 14	- 9	+ 2	5	+ 11	8	6.5
1093	252.15	+	26	-13	+03	-11	-12	0.2	8.3	- 10	- 12	- 17	- 20	- 15	- 5	5	+ 2	6	6
1096	253.07	+	12	-05	-01	-03	-06	0.2	8.3	- 3	- 6	- 6	- 10	- 7	+ 5	5	- 10	6	6.5
1097	253.58	+	35	-07	-03	-02	-09	0.3	8.3	- 2	- 2	- 10	- 12	- 11	- 18	5	- 4	7	6.5
1098	253.90	-	21	-03	-07	+04	-07	0.3	8.3	+ 4	- 8	+ 10	+ 20	- 6	+ 34	5	- 28	7	6
1100	254.46	+	39	-04	-13	+09	-11	2.6	9.3	+110	-137	+ 97	- 62	- 138	- 83	12	- 149	39	3
1101	254.61	+	23	-19	+01	-14	-18	0.3	8.3	- 19	- 25	- 25	- 18	- 24	- 2	5	+ 7	8	6
1102	254.95	+	16	-10	-03	-04	-11	0.2	8.3	- 5	- 13	- 9	- 14	- 13	+ 1	5	- 8	7	6.5
1103	254.99	+	15	-16	+04	-16	-13	0.5	8.3	- 37	- 32	- 40	- 8	- 30	+ 8	5	+ 17	9	3
1104	255.16	+	23	+16	+01	+08	+16	0.3	8.3	+ 12	+ 24	+ 5	- 28	+ 21	- 14	5	- 23	9	6
1105	255.66	+	22	-34	-03	-19	-35	0.5	8.3	- 42	- 75	- 45	- 8	- 76	+ 8	7	+ 23	18	5
1106	255.67	+	45	-10	+01	-07	-09	2.5	9.2	- 83	- 113	- 87	- 7	- 118	+ 20	10	+ 15	36	2
1107	255.89	+	14	+07	-06	+09	+04	0.5	8.3	+ 20	+ 8	+ 16	- 19	+ 7	- 6	5	- 38	7	2
1109	255.98	-	24	-22	+13	-24	-15	0.7	8.4	- 77	- 48	- 68	+ 46	- 45	+ 64	6	+ 36	14	2
1112	257.47	+	14	+11	-12	+16	+04	0.4	8.3	+ 30	+ 8	+ 26	- 21	+ 6	- 8	6	- 47	12	6
1113	257.51	+	35	-04	+00	-03	-04	0.2	8.3	- 3	- 4	- 10	- 32	- 10	- 18	5	- 6	6	6
1114	257.87	+	5	-09	-00	-06	-08	0.4	8.3	- 12	- 17	- 13	- 3	- 17	+ 12	6	- 9	12	6.5
1118	260.06	+	8	-10	+00	-07	-13	0.2	8.2	- 0	- 15	- 1	- 6	- 16	+ 8	5	- 16	3	2
1120	260.18	+	24	-04	+04	-06	-02	0.8	8.4	- 22	- 6	- 26	- 18	- 10	- 3	5	- 4	12	2
1122	260.23	+	30	-13	-10	-02	-18	0.8	8.4	- 7	- 64	- 12	- 32	- 62	- 18	6	- 16	21	6.5
1123	260.24	+	36	-02	+05	-06	+01	0.5	8.3	- 13	+ 2	- 19	- 33	- 5	- 18	5	- 3	7	2
1124	260.50	+	23	-10	+18	-21	+01	0.3	8.3	- 33	+ 2	- 37	- 17	0	- 1	5	+ 18	10	6
1125	260.61	+	25	+04	+06	-04	+07	0.4	8.3	- 7	+ 13	- 11	- 26	+ 8	- 11	5	- 9	6	2
1126	261.09	+	27	+15	+04	+04	+16	0.7	8.3	+ 12	+ 51	+ 7	- 37	+ 45	- 24	6	- 33	20	6
1128	262.05	+	41	+04	+05	-03	+06	1.1	8.4	- 14	+ 32	- 20	- 44	+ 24	- 29	5	- 14	16	2
1133	262.58	+	13	-20	+19	-27	-07	0.4	8.3	- 51	- 13	- 52	- 5	- 15	+ 12	5	+ 31	13	6
1134	262.71	+	24	-13	+10	-16	-06	0.4	8.3	- 34	- 12	- 37	- 19	- 13	- 3	5	+ 15	13	6
1135	262.77	+	18	+00	+07	-06	+04	0.6	8.3	- 19	+ 12	- 22	- 17	+ 8	- 2	5	- 5	18	6
1137	262.80	+	35	-02	+07	-07	-02	0.2	8.2	- 6	+ 2	- 10	- 34	- 3	- 19	5	- 5	3	2
1140	263.33	+	5	+03	+01	+01	+03	0.3	8.2	+ 2	+ 4	+ 1	- 6	+ 3	+ 9	5	- 19	8	6
1141	263.48	+	20	-03	+08	-09	+02	0.2	8.2	- 10	+ 2	- 12	- 19	- 2	- 4	5	- 4	4	2
1142	263.54	+	18	-33	+04	-21	-26	0.7	8.3	- 68	- 85	- 68	+ 3	- 87	+ 22	6	+ 38	22	6
1143	263.78	+	22	-27	+07	-23	-19	0.5	8.3	- 56	- 47	- 58	- 53	- 13	- 48	5	+ 34	17	6
1146	264.02	+	14	+22	+06	+08	+22	0.4	8.2	+ 14	+ 39	+ 12	- 20	+ 37	- 6	5	- 32	11	6
1147	264.06	+	11	+02	+04	-03	+04	1.0	8.4	- 13	+ 19	- 14	- 13	+ 16	+ 1	6	- 21	27	6
1151	264.32	+	20	-02	-07	+05	-06	1.4	8.4	+ 34	- 37	+ 33	- 18	- 39	- 13	6	- 77	39	6
1152	264.44	+	25	-04	-03	-06	-06	1.3	8.4	- 3	- 34	- 5	- 23	- 35	- 11	6	- 38	37	6
1154	264.98	+	26	-05	+07	-08	-08	0.4	8.2	- 18	- 1	- 20	- 24	- 4	- 9	5	- 2	7	2
1155	265.15	+	14	-11	-00	-06	-09	0.2	8.2	- 6	- 8	- 7	- 13	- 9	+ 2	5	- 9	5	6
1157	265.30	+	20	+00	+01	-00	+01	0.5	8.3	- 1	+ 3	- 3	- 20	+ 3	- 6	5	- 20	14	6
1159	265.65	+	22	+01	+08	-06	+06	0.4	8.2	- 10	+ 10	- 12	- 21	+ 10	- 6	5	- 8	11	6
1161	266.25	+	8	-03	+00	-02	-03	1.4	8.4	- 15	- 18	- 16	- 6	- 18	+ 6	5	- 33	21	2
1163	266.57	+	8	+17	+18	-04	+24	0.7	8.3	- 12	+ 80	- 13	- 13	+ 79	+ 2	5	- 15	20	6
1164	266.58	+	32	-20	+11	-23	-08	0.2	8.2	- 18	- 6	- 20	- 31	- 4	- 16	5	+ 6	5	6
1165	268.59	+	58	-24	-07	-10	-23	0.3	8.2	- 12	- 31	- 16	- 55	- 34	- 40	5	- 1	8	6
1166	268.79	+	26	-08	-06	-01	-10	0.9	8.3	- 5	- 41	- 2	- 10	- 27	- 40	5	- 25	25	6
1167	267.14	+	18	+01	+04	-03	+03	0.5	8.2	- 6	+ 7	- 7	- 18	+ 5	- 4	5	- 16	7	3
1169	267.37	+	35	-03	+02	-03	-00	1.7	8.4	- 27	- 4	- 29	- 34	- 2	- 19	5	- 20	47	6
1170	267.89	+	3	-15	-01	-09	-12	0.3	8.2	- 11	- 15	- 11	- 2	- 15	+ 13	5	- 7	4	3
1172	268.10	+	28	+23	-00	+14	+17	0.2	8.2	+ 15	+ 19	+ 14	- 30	+ 17	- 16	5	- 30	4	2
1173	268.23	+	7	+00	-06	+05	-04	0.3	8.2	+ 8	- 6	+ 8	- 7	- 6	+ 8	5	- 27	9	6
1174	268.68	+	7	-19	+09	-21	-08	0.6	8.2	- 62</td									

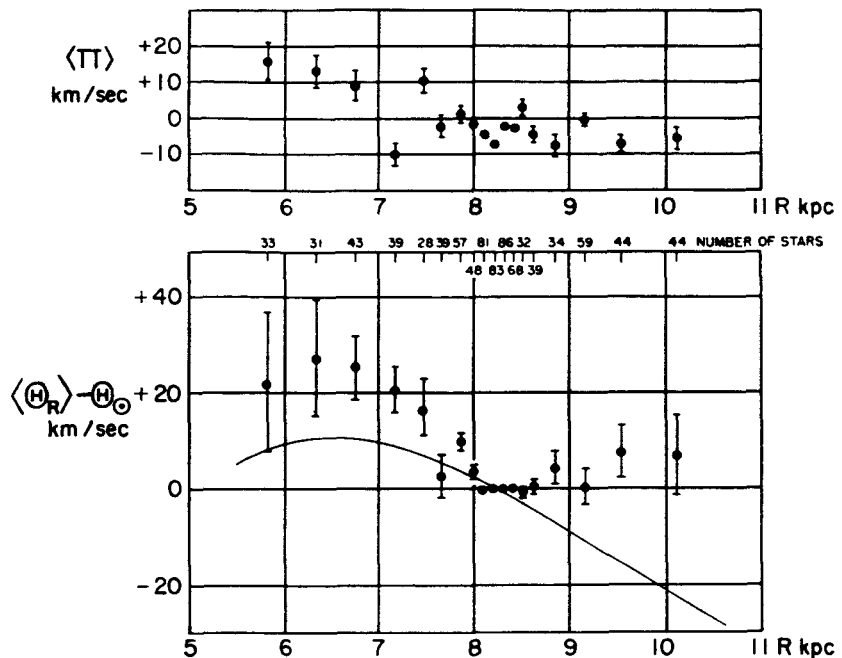
TABLE IV (continued)

Star No.	ℓ^{II}	ρ km/sec	μ_α 0.0000	μ_δ 0.000	μ_1 0.000	μ_b 0.000	r kpc	R kpc	T_1 km/sec	T_b km/sec	\dot{z} km/sec	$\dot{\nu}$ km/sec	\dot{s} km/sec	$\Theta - \Theta_s$ km/sec	Π km/sec	Source μ_α, δ
(1)	(2)	(3)	(4)	(5)	(6)	(7)	(8)	(9)	(10)	(11)	(12)	(13)	(14)	(15)	(16)	(17)
1194	275°89	+ 22	-04	+09	-09	+04	0.1	8.2	- 6	+ 3	- 3	- 22	+ 1	- 8 ± 5	- 10 ± 2	3
1195	276.17	+ 16	-12	+07	-13	-02	1.8	8.2	-113	- 16	-111	- 28	- 17	+ 4 ± 9	+ 53 ± 70	5
1197	276.87	+ 8	-03	-07	+03	-07	0.7	8.1	+ 9	- 25	+ 10	- 8	+ 5	+ 5 ± 6	- 40 ± 21	6
1198	276.89	+ 17	-03	+15	-11	+10	0.7	8.1	- 36	+ 34	- 34	- 18	+ 35	+ 1 ± 6	+ 5 ± 20	6
1199	277.30	+ 9	-05	-06	+01	-08	0.4	8.2	+ 1	- 15	+ 2	- 9	- 14	+ 5 ± 5	- 23 ± 6	3
1200	277.33	+ 2	-01	+06	-05	+03	0.2	8.2	- 5	+ 3	- 5	- 3	+ 3	+ 12 ± 5	- 11 ± 6	6, 5
1201	277.34	+ 5	+00	+03	-01	+02	0.4	8.2	- 2	+ 4	- 2	- 5	+ 4	+ 9 ± 5	- 19 ± 10	6
1202	277.53	+ 13	-13	-01	-08	-08	0.4	8.2	- 14	- 14	- 13	- 14	+ 1	+ 1 ± 5	- 7 ± 10	6, 5
1203	277.70	+ 23	-19	+09	-17	-04	0.2	8.2	- 12	- 3	- 9	- 24	- 6	- 9 ± 5	- 5 ± 3	1
1204	278.20	+ 16	+03	+07	-02	+07	0.3	8.2	- 2	+ 11	0	- 16	+ 12	- 1 ± 5	- 19 ± 5	1
1205	278.41	+ 6	-22	+05	-17	-08	0.4	8.2	- 29	- 14	- 28	- 9	- 15	+ 6 ± 5	+ 8 ± 8	11, 6, 5
1206	279.15	+ 23	-09	+01	-07	-04	0.2	8.2	- 7	- 4	- 3	- 24	- 3	- 9 ± 5	- 13 ± 3	8
1207	279.18	+ 12	-23	-09	-11	-20	0.3	8.2	- 13	- 25	- 11	- 15	- 24	0 ± 5	- 6 ± 4	1
1208	279.69	+ 3	+12	+09	+05	+14	2.4	8.1	+ 54	+155	+ 51	+ 18	+155	+ 4 ± 8	- 131 ± 34	3
1209	279.84	+ 7	+11	-00	+09	+06	0.6	8.1	+ 27	+ 17	+ 28	- 1	+ 17	+ 11 ± 6	- 56 ± 18	6
1210	280.04	- 6	-17	-10	-05	-17	2.9	8.2	- 75	-232	- 74	- 10	- 232	+ 14 ± 20	- 16 ± 108	5
1211	280.23	+ 17	-45	+12	-31	-15	0.2	8.2	- 28	- 14	- 25	- 19	- 16	+ 4 ± 5	+ 10 ± 5	1
1212	280.24	- 19	+15	+09	+07	+15	1.9	8.1	+ 62	+136	+ 56	+ 38	+134	+ 30 ± 14	- 127 ± 72	5
1213	280.73	+ 17	08	+02	-06	-03	0.4	8.1	- 10	- 5	- 7	- 18	- 7	- 3 ± 5	- 13 ± 10	6, 5
1214	281.73	+ 9	-05	+04	-05	+01	0.4	8.1	- 9	+ 1	- 7	- 11	+ 2	+ 4 ± 5	- 13 ± 5	1
1215	282.98	+ 10	-12	+04	-10	-02	0.2	8.2	- 9	- 2	- 6	- 11	- 2	+ 3 ± 5	- 9 ± 5	6, 5
1216	283.87	+ 10	-04	+04	-05	+02	0.4	8.1	- 9	+ 3	- 7	- 12	+ 4	+ 3 ± 6	- 14 ± 11	6, 5
1217	284.27	- 2	03	+01	-02	-01	0.2	8.1	- 3	- 1	- 3	+ 1	- 1	+ 16 ± 5	- 14 ± 6	6, 5
1218	284.54	+ 18	+10	-04	+09	+00	0.5	8.1	+ 19	+ 1	+ 23	- 13	- 0	0 ± 6	- 46 ± 13	6, 5
1220	285.16	- 2	+06	+03	+02	+05	2.1	7.9	+ 21	+ 45	+ 20	+ 6	+ 45	+ 5 ± 21	- 89 ± 77	5
1221	285.18	+ 32	-15	+02	-12	-04	0.4	8.1	- 21	- 8	- 12	- 37	- 7	- 22 ± 6	- 7 ± 11	6, 5
1222	285.30	+ 11	-03	-00	-02	-02	0.4	8.1	- 3	- 3	- 0	- 11	- 4	+ 3 ± 5	- 20 ± 5	2
1223	285.33	- 18	+06	-04	+06	-01	2.5	7.9	+ 70	- 14	+ 63	+ 37	- 12	+ 17 ± 26	- 152 ± 92	5
1225	285.63	+ 20	-17	-07	-08	-13	0.5	8.1	- 22	- 34	- 16	- 26	- 33	- 11 ± 6	- 8 ± 15	6, 5
1227	285.81	- 8	+05	-03	+05	-01	2.8	7.9	+ 68	- 9	+ 64	+ 26	- 9	+ 2 ± 22	- 156 ± 76	6, 5
1228	285.85	0	-04	-12	+09	-09	2.5	7.9	+107	-106	+103	+ 29	- 106	- 3 ± 20	- 187 ± 70	6, 5
1239	286.23	- 10	+11	-05	+10	-00	2.0	7.9	+ 97	- 2	+ 90	+ 37	- 2	+ 19 ± 22	- 163 ± 74	5
1242	287.10	- 2	+09	-01	+07	+02	1.9	7.9	+ 62	+ 21	+ 59	+ 20	+ 21	+ 12 ± 17	- 125 ± 52	6, 5
1243	287.18	+ 26	-18	+05	-14	-03	0.1	8.2	- 10	- 2	- 1	- 28	- 3	- 13 ± 5	- 12 ± 3	2
1244	287.18	- 27	-29	+15	-29	+03	3.2	7.9	-439	+ 44	- 428	- 101	+ 42	+ 65 ± 40	+336 ± 128	5
1246	287.67	- 27	+03	+05	-00	+05	2.0	7.8	- 1	+ 51	- 9	+ 25	+ 52	+ 32 ± 10	- 64 ± 27	5
1247	287.94	- 29	+09	+01	+06	+04	1.9	7.8	+ 56	+ 35	+ 44	+ 46	+ 34	+ 41 ± 23	- 117 ± 69	5
1249	288.18	- 11	-08	+04	-07	+01	0.3	8.1	- 9	+ 1	- 12	+ 8	+ 1	+ 23 ± 5	- 6 ± 4	3
1250	288.25	- 9	+00	-05	+02	-05	2.8	7.8	+ 32	- 59	+ 27	+ 19	- 59	+ 7 ± 7	- 119 ± 99	5
1251	289.04	+ 2	-24	-12	-13	-19	0.6	8.0	- 37	- 54	- 33	- 16	- 54	0 ± 8	+ 8 ± 17	6, 5
1252	289.50	+ 26	-18	+14	-17	+07	0.2	8.1	- 15	+ 6	- 5	- 29	+ 4	- 14 ± 5	- 10 ± 4	1
1253	289.57	+ 24	-15	+13	-15	+06	0.2	8.1	- 13	- 4	- 4	- 28	+ 3	- 13 ± 5	- 11 ± 3	3
1254	289.60	+ 24	-19	+10	-15	+03	0.2	8.1	- 18	+ 3	- 8	- 20	+ 1	- 14 ± 5	- 8 ± 4	2
1255	289.62	+ 8	-04	+08	-06	+06	0.2	8.1	- 5	+ 5	- 2	- 9	+ 4	+ 5 ± 5	- 13 ± 3	1
1256	289.75	- 9	-27	-09	-09	-16	0.2	8.1	- 9	- 17	- 13	+ 7	- 15	+ 22 ± 5	- 4 ± 6	6
1257	289.95	+ 14	-30	-01	-25	-10	0.1	8.2	- 11	- 5	- 6	- 17	- 3	- 2 ± 5	- 7 ± 3	1
1258	289.96	+ 16	-23	+06	-16	-02	0.2	8.1	- 17	- 2	- 11	- 21	- 3	- 6 ± 5	- 5 ± 4	1
1259	290.12	- 1	-38	+03	-23	-09	0.5	8.0	- 60	- 23	- 58	- 18	- 22	8 ± 33	- 17 ± 6	6
1260	290.83	+ 17	+01	-05	+02	-04	0.3	8.1	+ 3	- 6	+ 9	- 15	- 6	0 ± 6	- 26 ± 10	5, 6
1261	291.73	- 10	-11	-04	-08	-07	2.3	7.7	- 85	- 74	- 80	- 27	- 74	- 1 ± 33	+ 11 ± 81	5
1262	292.36	- 9	+15	-00	+10	+04	2.1	7.7	+101	+ 35	+ 90	+ 47	+ 35	+ 27 ± 31	- 167 ± 74	5
1263	292.78	+ 4	+05	-06	+05	-04	2.4	7.6	+ 60	- 51	+ 55	+ 23	+ 1	+ 8 ± 27	- 136 ± 63	6
1264	292.86	+ 9	-17	+05	-14	+01	0.3	8.1	- 17	+ 1	- 12	- 15	+ 1	0 ± 5	- 5 ± 5	1
1265	293.31	- 3	-3	+09	-06	+08	3.3	7.5	+124	- 60	+113	+ 51	- 60	- 8 ± 38	- 226 ± 88	6, 5
1266	293.93	+ 2	+08	+05	+03	+06	2.8	7.5	+ 44	+ 83	+ 42	+ 13	+ 82	- 4 ± 17	- 131 ± 36	2
1267	293.97	+ 9	-09	+04	-08	+02	0.4	8.0	- 15	+ 4	- 10	- 14	+ 4	0 ± 5	- 10 ± 6	1
1268	294.50	+ 7	-36	-14	-13	-13	0.4	8.0	- 27	- 24	- 23	- 14	- 25	+ 2 ± 5	+ 3 ± 2	2
1269	294.78	- 14	-26	+05	-17	-00	3.3	7.4	-262	- 4	- 244	- 97	- 3	+ 1 ± 43	+160 ± 92	6
1270	294.78	- 16	+07	-01	+05	+00	2.1	7.6	+ 45	+ 3	+ 34	+ 33	+ 3	+ 29 ± 25	- 109 ± 54	6, 5
1271	295.21	- 3	-03	-13	+02	-13	3.3	7.4	+ 25	- 205	+ 21	+ 16	- 204	- 3 ± 54	- 128 ± 114	5
1272	295.62	- 17	+07	+13	+02	+14	2.8	7.4	+ 24	+181	+ 15	+ 25	+181	+ 17 ± 45	- 109 ± 94	5
1273	295.89	- 2	-07	-01	-04	-02	3.0	7.4	- 64	- 30	- 58	- 26	- 30	- 8 ± 20	- 31 ± 39	2
1274	295.97	- 37	+27	+13	+16	+17	2.4	7.5	+184	+194	+ 149	+116	+194	+ 70 ± 42	- 252 ± 85	5
1275	296.17	+ 37	-28	-04	-17	-08	0.1	8.2	- 9	+ 5	+ 8	- 37	- 6	- 22 ± 5	- 21 ± 4	6, 5
1276	296.75	+ 16	-25	-05	-16	-08	0.3	8.1	- 20	- 11	- 11	- 23	- 11	- 8 ± 5	- 6 ± 5	1
1277	296.78	+ 21	-36	-31	-17	-17	0.1	8.1	- 19	- 10	- 7	- 28	- 6	- 14 ± 5	- 7 ± 4	1
1278	297.64	+ 16	-14	+11	-11	+09	0.3	8.1	- 18	+ 14	- 8	- 23	+ 14	- 8 ± 5	- 10 ± 5	1
1279	298.15	+ 2	-06	-01	-04	-02	2.4	7.4	- 45	- 19	- 39	- 23	- 19	- 9 ± 43	- 32 ± 80	5
1280	298.23	+ 26	-38	-10	-28	-14	0.2	8.1	- 22	- 11	- 7	- 34	- 9	- 19 ± 5	- 7 ± 4	2
1281	298.47	- 4	-25	-05	-19	-08	3.2	7.2	-288	- 114	- 251	- 142	- 114	- 41 ± 60	+188 ± 111	5
1283	298.60	+ 2	+20	-18	+16	-16	2.0	7.5	+156	-149	+138	+ 72	-149	+ 44 ± 44	-215 ± 69	5
1284	298.93	- 7	-00	+01	-00	+01	3.2	7.2	- 3	+ 15	- 6	+ 4	+ 15	0 ± 22	- 94 ± 39	2
1286	299.23	+ 9	-25	-17	-13	-19	0.3	8.0	- 21	- 31	- 15	- 16	- 32	- 1 ± 43	- 4 ± 9	6
1287	299.33	+ 19	-52	-12	-33	-16	0.1	8.1	- 22	- 11	- 10	- 27	- 11	- 9 ± 43	- 32 ± 80	5
1288	300.12	+ 27	-48	-20	-31	-23	0.3	8.1	- 42	- 32	- 23	- 44	- 32	- 29 ± 7	- 7 ± 3	2

TABLE IV (*continued*)

Star No.	ℓ^{11}	ρ km/sec	μ_α 0°0000	μ_δ 0°000	μ_α 0°000	μ_δ 0°000	r	R kpc	T_t km/sec	T_b km/sec	\dot{x} km/sec	\dot{y} km/sec	\dot{z} km/sec	$\Theta - \Theta_0$ km/sec	Π km/sec	Source $\mu\alpha, \delta$		
(1)	(2)	(3)	(4)	(5)	(6)	(7)	(8)	(9)	(10)	(11)	(12)	(13)	(14)	(15)	(16)	(17)		
1313	304°68	- 28	- 00	- 08	- 01	- 08	0.7	7.8	- 2	- 25	- 18	+ 23	- 24	+ 38	± 7	- 10 ± 8	2	
1314	305.47	- 28	- 02	- 06	- 02	- 05	1.1	7.6	- 10	- 26	- 24	+ 17	- 26	+ 32	24	- 15	34	
1315	305.52	- 11	+ 04	- 07	+ 02	- 07	1.2	7.6	+ 11	- 42	+ 2	+ 16	- 42	+ 27	20	- 45	28	
1316	305.61	- 7	- 19	+ 04	- 12	+ 05	2.0	7.2	- 117	+ 47	- 99	- 63	+ 47	- 33	45	+ 48	63	
1317	305.80	- 8	+ 07	- 01	+ 06	- 02	1.2	7.6	+ 35	- 9	+ 25	+ 26	- 10	+ 34	27	- 68	37	
1319	305.88	- 71	- 24	- 02	- 16	- 01	2.9	6.9	- 224	- 7	- 223	- 73	- 6	+ 4	67	+ 147	92	
1321	306.70	- 7	+ 19	- 15	+ 12	- 17	0.4	8.0	+ 21	- 29	+ 13	+ 17	- 29	+ 31	5	- 32	6	
1322	306.71	+ 26	- 25	- 10	- 19	- 08	0.2	8.1	- 17	- 7	+ 2	- 31	- 6	- 16	5	- 16	4	
1323	306.76	- 22	+ 02	- 07	+ 00	- 07	2.0	7.2	+ 5	- 69	- 8	+ 19	- 69	+ 27	45	- 57	61	
1327	307.06	- 12	+ 09	- 03	+ 05	- 04	0.5	7.9	+ 14	- 10	+ 4	+ 18	- 10	+ 32	10	- 28	13	
1328	307.08	- 2	+ 01	+ 10	+ 02	+ 10	1.4	7.4	+ 14	+ 66	+ 5	+ 16	+ 65	+ 26	13	- 54	17	
1332	308.52	- 18	- 39	+ 14	- 23	+ 18	2.9	6.8	- 311	+ 252	- 251	- 184	+ 252	- 92	73	+ 211	92	
1334	309.23	- 14	- 34	- 00	- 23	+ 05	1.6	7.3	- 173	+ 34	- 143	- 99	+ 34	- 63	21	+ 108	26	
1335	309.97	- 48	- 05	- 03	- 05	- 02	0.7	7.8	- 16	- 8	- 42	+ 26	- 12	+ 42	8	+ 14	8	
1336	310.19	+	6	- 15	- 14	- 16	0.1	8.1	- 11	- 8	- 4	- 12	- 7	+ 3	4	- 9	4	
1337	311.27	- 20	- 00	+ 01	- 00	+ 01	0.3	8.0	0	+ 1	- 13	+ 15	+ 3	+ 30	5	- 5	5	
1339	311.77	- 12	- 23	- 19	- 22	- 14	0.1	8.1	- 12	- 8	- 17	+ 1	- 8	+ 16	4	+ 4	4	
1340	312.02	- 26	+ 03	- 04	+ 01	- 05	1.6	7.2	+ 10	- 37	- 9	+ 25	- 33	+ 36	40	- 43	45	
1341	312.16	+ 39	+ 09	- 02	+ 06	- 04	1.9	7.1	+ 54	- 39	+ 14	+ 64	- 40	+ 69	37	- 83	41	
1342	312.26	+	1	+ 08	+ 15	+ 10	+ 12	2.3	6.9	+ 111	+ 132	+ 80	+ 77	+ 132	+ 60	24	- 163	27
1343	312.73	- 14	+ 00	- 20	- 08	- 18	0.5	7.9	- 20	- 45	- 28	+ 1	- 43	+ 17	11	+ 6	12	
1344	313.25	+	1	- 05	+ 08	+ 01	+ 09	0.7	7.8	+ 3	+ 27	+ 6	+ 1	+ 27	+ 12	13	- 30	14
1345	313.86	- 33	- 54	+ 20	- 25	+ 23	2.0	7.0	- 240	+ 307	- 183	- 156	+ 309	- 107	46	+ 153	47	
1346	314.13	+ 18	- 25	- 10	- 22	- 04	0.3	8.0	- 29	- 5	- 10	- 32	- 4	- 17	7	- 6	7	
1348	314.29	+ 8	- 35	- 28	- 31	- 16	0.7	7.7	- 107	- 55	- 75	- 77	- 55	- 58	18	+ 54	18	
1349	315.03	- 21	- 15	- 22	- 18	- 15	0.3	8.0	- 22	- 18	- 31	+ 1	- 16	+ 16	7	+ 16	7	
1350	315.26	- 5	- 21	- 06	- 16	+ 01	0.4	7.9	- 27	+ 2	- 23	- 16	+ 2	- 1	9	+ 5	9	
1351	316.71	- 1	+ 04	- 05	+ 01	- 06	0.3	8.0	+ 1	- 9	- 1	+ 2	- 8	+ 16	7	- 16	7	
1352	318.40	- 8	- 07	- 02	- 05	+ 01	0.5	7.9	- 11	+ 1	- 13	- 3	+ 2	+ 12	10	- 6	9	
1353	318.58	- 5	+ 00	- 05	- 02	- 04	0.6	7.8	- 5	- 12	- 7	- 1	- 13	+ 13	13	- 16	12	
1354	318.93	- 2	- 28	- 10	- 29	+ 01	0.3	8.0	- 46	+ 2	- 32	- 33	+ 2	- 18	7	+ 16	6	
1355	319.18	- 12	- 11	- 12	- 13	- 06	0.3	8.0	- 15	- 8	- 19	- 3	- 7	+ 12	7	+ 4	6	
1357	319.69	+ 88	- 08	- 03	- 06	+ 00	0.7	7.7	- 20	+ 1	+ 54	- 72	- 3	- 61	8	+ 73	7	
1358	320.13	+ 14	- 22	- 12	- 25	- 02	0.1	8.1	- 16	- 1	- 1	- 21	+ 1	- 6	5	- 14	5	
1359	320.13	- 6	- 01	+ 01	+ 00	+ 01	1.8	6.9	+ 2	+ 9	- 3	+ 5	+ 9	+ 15	20	- 47	17	
1360	321.22	- 61	+ 07	- 00	+ 04	- 03	1.7	6.9	+ 35	- 23	- 26	+ 66	- 21	+ 80	39	- 31	31	
1361	321.24	- 17	- 14	- 42	- 32	- 29	0.1	8.1	- 12	- 11	- 21	- 21	+ 17	4	+ 9	4	6.5	
1362	323.08	- 2	+ 13	- 17	+ 02	- 21	0.6	7.7	+ 7	- 62	+ 7	+ 3	- 62	+ 17	15	- 29	12	
1363	325.33	+ 17	- 19	- 15	- 25	- 03	0.1	8.1	- 14	- 2	- 2	- 21	+ 1	- 7	4	- 18	4	
1364	326.79	- 2	+ 08	- 02	+ 02	- 05	0.5	7.8	+ 6	- 12	+ 1	+ 6	- 12	+ 20	7	- 20	6	
1369	327.94	- 40	+ 10	+ 18	+ 18	+ 08	2.6	6.1	+ 222	+ 100	+ 85	+ 209	+ 101	+ 190	88	- 193	56	
1370	328.09	- 13	+ 09	- 02	+ 05	- 07	0.3	7.9	+ 9	- 11	- 6	+ 14	- 12	+ 29	9	- 10	7	
1371	328.58	+ 8	+ 28	+ 10	+ 25	- 08	2.1	6.5	+ 244	- 80	+ 131	+ 206	- 80	+ 191	73	- 213	45	
1372	329.23	+ 4	- 10	- 07	- 13	+ 00	0.1	8.1	- 6	0	0	2	- 10	+ 13	4	+ 2	5	
1373	329.77	- 16	+ 05	- 06	- 02	- 07	0.0	8.2	0	0	- 14	+ 8	+ 2	+ 23	3	+ 3	4	
1375	331.28	- 38	- 17	- 26	- 29	- 08	1.5	6.9	- 209	- 56	- 135	- 164	- 55	- 137	56	+ 116	31	
1376	331.88	+	6	- 04	- 19	- 18	0.2	8.0	- 17	- 9	- 4	- 17	- 9	- 2	4	- 9	5	
1377	333.67	0	- 02	+ 25	+ 17	+ 18	1.5	6.9	+ 124	+ 132	+ 63	+ 107	+ 131	+ 113	54	- 106	27	
1378	335.99	- 12	+ 03	- 23	- 14	- 18	0.1	8.1	- 7	- 9	- 14	2	- 10	+ 13	4	+ 2	5	
1379	336.65	- 18	+ 19	- 02	+ 11	- 15	3.2	5.4	+ 166	- 229	+ 44	+ 162	- 229	+ 154	85	- 143	37	
1382	336.78	+ 28	- 08	- 02	- 07	+ 05	0.5	7.8	- 14	- 10	+ 21	- 24	+ 8	- 10	7	- 36	8	
1383	337.25	- 19	+ 11	- 02	+ 07	- 10	1.1	7.2	+ 35	- 50	- 3	+ 39	- 51	+ 53	15	- 23	8	
1384	338.19	+	5	+ 13	+ 05	+ 14	- 07	1.0	7.3	+ 62	- 30	+ 29	+ 55	- 30	+ 68	26	- 53	12
1385	338.56	- 39	- 11	- 18	- 21	- 03	1.4	6.9	- 143	- 23	- 89	- 119	- 22	- 98	42	+ 70	17	
1387	339.12	- 1	- 16	- 27	- 32	- 07	0.2	8.0	- 29	- 6	- 10	- 27	- 6	- 12	5	- 2	1	
1388	339.38	+	5	- 03	- 04	- 05	- 01	1.5	6.8	- 34	- 4	- 7	- 34	- 3	- 20	21	- 19	9
1389	340.39	+	2	- 03	- 17	- 14	- 09	0.4	7.8	- 27	- 17	- 6	- 27	- 17	- 12	7	- 8	5
1391	340.57	- 12	+ 27	+ 20	+ 33	- 10	1.6	6.7	+ 245	- 75	+ 66	+ 236	- 74	+ 244	53	- 112	19	
1392	340.76	- 2	- 25	- 65	- 68	- 14	0.1	8.1	- 39	- 8	- 16	- 36	- 8	- 21	6	+ 4	5	
1393	342.02	- 19	- 08	- 13	- 16	- 01	0.3	7.9	- 24	- 1	- 25	- 17	+ 1	- 2	6	+ 12	5	
1394	342.64	- 15	+ 10	+ 01	+ 07	- 08	0.5	7.7	+ 17	- 19	- 11	+ 22	- 17	+ 37	15	- 4	7	
1395	343.03	- 26	+ 10	+ 02	+ 09	- 08	0.4	7.9	+ 15	- 13	- 20	+ 22	- 14	+ 37	10	+ 7	6	
1399	343.31	- 36	+ 05	- 12	- 06	- 12	1.4	6.9	- 36	- 81	- 43	- 25	- 81	- 8	38	+ 21	12	
1400	343.34	- 28	- 01	+ 10	+ 07	+ 07	1.4	6.9	+ 47	+ 45	- 14	+ 53	+ 44	+ 68	38	- 12	12	
1401	343.35	- 18	- 06	+ 03	- 02	+ 07	1.4	6.9	- 11	+ 44	- 21	- 6	+ 43	+ 10	38	- 2	6	
1403	343.45	- 6	+ 00	- 02	- 01	- 02	1.4	6.9	- 9	- 11	- 8	- 7	- 11	+ 4	3	- 15	12	
1404	343.45	- 24	+ 17	- 33	- 13	- 36	1.4	6.9	- 86	- 236	- 43	- 77	- 236	- 61	39	+ 24	13	
1405	343.47	- 16	- 14	+ 15	+ 02	+ 21	1.4	6.9	+ 12	+ 139	- 15	+ 17	+ 138	+ 32	38	- 10	14	
1411	343.62	- 63	+ 08	+ 05	+ 10	- 04	1.4	6.9	+ 65	- 27	- 41	+ 79	- 29	+ 96	39	+ 13	12	
1412	343.63	- 17	+ 08	- 06	- 00	- 11	1.9	6.4	- 1	- 98	- 23	+ 5	- 96	+ 21	52	- 7	6	
1413	344.09	- 138	- 08	- 06	- 10	+ 03	1.4	6.9	- 66	+ 18	- 151	- 26	+ 14	- 3	39	+ 129	12	
1414	344.81	- 7	- 02	+ 18	+ 13	+ 13	1.7	6.5	+ 105	+ 104	+ 18	+ 104	+ 103	+ 116	50	- 52	14	
1417	345.94	0	- 04	- 11	- 12	- 04	0.2	8.0	- 12	- 4	- 2	- 11	- 3	+ 4	3	- 10	5	

FIG. 5. *Upper plot.* The variation of $\langle \Pi \rangle$ as a function of distance from the center of the galaxy, for 888 stars. The weighted mean and the probable error of the weighted mean is indicated for each distance group. *Lower plot.* The variation of $\langle \Theta \rangle - \Theta_0$ for 888 stars, as a function of distance from the center of the galaxy. The weighted mean and the probable error of the weighted mean is shown for each point. The number of stars in each point is shown at the upper edge of the drawing. The solid curve represents the rotation curve for the gaseous component of the galaxy from the radio model of the galaxy (Kwee, Muller, and Westerhout 1954; Schmidt 1956).



(a) *MK luminosity calibration.* To first order in r/R , for a constant error ΔM in the absolute magnitude calibration of the MK luminosity classification, there will be an error in each computed Θ_i from Eqs. (7), (8), and (11), given by

$$\Delta\Theta = -0.46\Delta M [T_i \cos l^{\text{II}} + (r/R) \sin l^{\text{II}} \times (-2T_i \sin l^{\text{II}} + \rho \cos l^{\text{II}} + \dot{x}_0)]. \quad (21)$$

To this same degree of approximation, for the Oort model

$$T_i = r(A \cos 2l^{\text{II}} + B). \quad (22)$$

The corresponding error in the distance of each star is given by

$$\Delta r = -0.46r\Delta M. \quad (23)$$

Toward the center and anticenter of the galaxy,

$$\Delta\Theta = \mp 0.46r\Delta M(A + B). \quad (24)$$

The negative sign is for $l^{\text{II}}=0^\circ$, the positive sign for $l^{\text{II}}=180^\circ$. Hence a positive ΔM , i.e., stars intrinsically fainter, will decrease the distance of each star from the sun. It will also decrease the values of $\langle \Theta \rangle - \Theta_0$ for the inner regions of the galaxy, but raise the rotation curve in the outer regions. Conversely, a negative value of ΔM , i.e., stars intrinsically brighter, will lower the outer rotation curve, but raise the inner parts. The impossibly large value of $\Delta M = -3^m 0$ is necessary to make the computed rotation curve for large R coincide with the radio curve; this would raise the inner parts of the curve approximately 30 km/sec. Toward $l^{\text{II}}=90^\circ$ and 270° , a value of $\Delta M = \pm 0^m 5$ will result in $\langle \Delta\Theta \rangle \approx \mp 2$ km/sec or less.

Similar arguments may be applied to determine the effects of a constant error in the correction for space

absorption. If the stars are actually closer, and the interstellar absorption has not been fully accounted for, then the effect on the rotation curve is the same as if the stars were actually fainter; the inner part is lowered, but the outer portion raised. If the ratio of total to selective absorption is equal to 3.2 (Blanco and Lennon 1961), then $\Delta M \approx 0^m 1$ for this sample of stars. In this case, $\Delta\Theta \approx 0.46$ km/sec for $r = 1$ kpc and $\cos l^{\text{II}} = 1$; the change in $\langle \Theta \rangle$ is negligible.

The calibration of the MK luminosity classification is a question of continuing interest; Petrie (1962) has recently restated his position. However, it appears from the derived rotation curve that a constant error in the luminosity calibration or in the procedure of accounting for interstellar absorption will not be sufficient to make the optical and radio curves coincide. A correction which will improve the agreement of the inner portions will decrease the coincidence elsewhere, and vice versa. As pointed out by Munch and Munch (1960), there is always the possibility that stars formed in different regions of the galaxy may have different intrinsic luminosities. Similarly, there is the possibility that the factor 3 for the ratio of total to selective absorption is not constant around the galactic plane (Sharpless 1952),

TABLE V. Corrections to N30 proper-motion system for a mean N30-FK4 system.

l^{II}	$\Delta\mu_l$
280°	0.000
290	-0.002
310	-0.002
325	-0.004
340	-0.003
350	-0.003
10°	0.000

TABLE VI. Values of $\langle \Theta \rangle - \Theta_0$ for various samples of stars.

Midpoint of distance interval R kpc	Entire sample $\langle \Theta \rangle - \Theta_0$ km/sec	No. stars (888)	No Lick radial velocities	No. stars (680)	No Lick or assumed class V	No. stars (575)	μ^{II}	No. stars (454)	μ^{II}	No. stars (434)
			$\langle \Theta \rangle - \Theta_0$ km/sec							
5.80	+22.1±14.6	33	- 6.5±44.4	8	- 6.5±44.4	8	+19.9±14.7	32	...	1
6.35	+27.4 12.3	31	+29.1 20.3	6	+29.1 20.3	6	+21.4 13.1	28	...	3
6.75	+25.9 6.7	43	+20.2 9.1	20	+20.2 9.1	20	+33.2 9.0	24	+17.9±10.1	19
7.15	+20.9 4.9	39	+21.7 5.3	25	+23.2 5.6	23	+11.9 6.7	22	+30.9 6.9	17
7.45	+17.0 5.6	28	- 0.8 5.9	16	- 0.8 5.9	16	+18.2 8.9	16	+15.1 4.8	12
7.65	+ 2.7 4.4	39	-11.0 5.4	21	-11.0 5.4	21	+10.5 4.5	26	-12.5 9.1	13
7.85	+ 9.9 1.5	57	+ 9.7 1.7	44	+ 9.6 1.7	39	+ 4.8 1.8	29	+15.6 2.3	28
8.0	+ 3.6 1.2	48	+ 3.8 1.2	46	+ 1.8 1.4	32	+ 3.8 1.4	31	+ 3.3 2.2	17
8.1	- 0.3 1.0	81	- 0.3 1.0	80	- 0.9 1.1	64	- 0.1 1.7	33	- 0.4 1.2	48
8.2	+ 0.1 0.9	83	+ 0.1 0.9	83	+ 0.1 1.1	64	+ 3.7 1.1	32	- 2.0 1.3	51
8.3	0.0 0.9	86	0.0 0.9	86	+ 0.4 1.0	67	+ 0.1 1.1	43	- 0.2 1.4	43
8.4	+ 0.1 1.1	68	- 0.3 1.1	61	- 2.6 1.0	48	+ 0.4 1.3	31	- 0.1 1.6	37
8.5	- 0.7 1.7	32	- 0.5 1.7	27	- 2.7 2.2	19	- 1.8 4.1	10	- 0.3 1.7	22
8.65	+ 0.9 1.9	39	+ 0.6 1.8	38	- 0.2 2.0	32	+ 2.6 2.4	19	- 1.2 2.9	20
8.85	+ 4.8 3.9	34	+ 5.8 4.6	26	+ 8.9 4.5	25	+12.3 6.2	18	- 7.9 3.3	16
9.15	+ 0.8 3.5	59	- 1.7 4.3	37	- 1.6 4.3	36	- 0.2 6.4	20	+ 1.5 4.2	39
9.55	+ 7.9 5.3	44	+ 9.0 5.9	32	+ 6.4 6.1	31	+14.5 8.1	20	- 1.0 6.9	24
10.30	+ 7.0± 8.5	44	+13.2±10.9	24	+13.2±10.9	24	+11.4±12.3	20	- 3.3±12.7	24

or even that the method of determining absorption corrections from $B-V$ measures is not completely satisfactory for highly reddened early-type stars.

If the early-type stars toward the center of the galaxy are intrinsically fainter than those toward the anticenter, or if the absorption toward the center of the galaxy is actually greater than computed, and less toward the anticenter, then the stellar and gaseous rotation curves would be more in agreement. What is needed is some method, independent of spectroscopic and color measures, to determine if the stars at the limits of this sample, i.e., toward the center and anticenter, are actually equally distant from the sun. This is not possible at present.

(b) *The proper-motion system.* To investigate effects of possible systematic errors in the N30 proper-motion system, the proper motions of these stars have been examined on a mean N30-FK4 system. From FK4 proper motions communicated in advance of publication to the U.S. Naval Observatory by the Astronomischen Rechen-Institut, and kindly made available by F. P. Scott, differences were formed between proper motions of 1532 stars common to N30 and FK4. Mean differences were formed for 144 zones, two hours wide in right ascension and 15° wide in declination. Differences between the two systems are small for stars in the northern sky. At southern declinations, especially south of -30° , the differences become large enough to affect the kinematical interpretations of proper motions observed for that region of the sky.

The corrections to be added to the N30 proper motions for a mean N30-FK4 system are tabulated in Table V, for $\mu^{\text{II}} \geq 280^\circ$. These values have been estimated visually from the right ascension-declination comparison. At all other longitudes, $\Delta\mu_i \leq 0.001$, and has been neglected. From Eqs. (7), (8), and (11):

$$\Delta\Theta = kr\Delta\mu_i [\cos\mu^{\text{II}} - (r/R) \sin^2\mu^{\text{II}}], \quad (25)$$

for each 4th-quadrant star. Stars with $\mu^{\text{II}} > 280^\circ$ and $r \geq 1$ kpc will in general have $R \leq 7.8$ kpc. Hence only points with $R \leq 7.8$ kpc will be altered in the rotation curve. But over two-thirds of the stars in this distance range are in the 1st, not the 4th quadrant, so the changes in the mean points will be slight. At each distance, $R=6.3, 6.7, 7.1$, and 7.3 kpc, $\langle \Theta \rangle - \Theta_0$ will be lowered less than 5 km/sec. All other mean points will remain unchanged.

(c) *The radial velocities.* From Eqs. (7), (8), and (11),

$$\Delta\Theta = \Delta\rho \sin\mu^{\text{II}} [1 + (r/R) \cos\mu^{\text{II}}]. \quad (26)$$

For a constant error $\Delta\rho$ in the observed radial velocities, all stars, $\mu^{\text{II}} < 180^\circ$, will have values of $\langle \Theta \rangle - \Theta_0$ consistently positive or consistently negative with respect to stars with $\mu^{\text{II}} > 180^\circ$, depending on the sign of $\Delta\rho$. However, no such difference is noted.

To substantiate these conclusions, several determinations of the mean rotation curve were made, in addition to that plotted in Fig. 5. These include:

- (1) a solution with 454 stars, $\mu^{\text{II}} \leq 180^\circ$,
- (2) a solution with 434 stars, $\mu^{\text{II}} > 180^\circ$,
- (3) a solution with 680 stars, all Lick radial-velocity stars omitted,
- (4) a solution with 575 stars, all Lick and assumed luminosity class V stars omitted,
- (5) a preliminary solution (Rubin *et al.* 1962) with 777 stars, calibrated on the older Johnson and Hiltner (1956) calibration, with normal colors taken from Hiltner (1956). The results of solutions 1-4 are listed in Table VI. Note that although the scatter of the mean points is sometimes large, the general form of the rotation curve is similar in all cases.

For a rotation curve of the general form found here, a modified form of the usual Oort double sine in the observed radial velocities would be expected. In the 1st

TABLE VII. Values of $\langle \Pi \rangle$ for various samples.

Midpoint of distance interval R kpc	Entire sample $\langle \Pi \rangle$ km/sec	No. stars (888)	No Lick radial velocities $\langle \Pi \rangle$ km/sec	No. stars (680)	No Lick or assumed class V $\langle \Pi \rangle$ km/sec	No. stars (575)
5.80	+15.5±5.5	33	+16.2±13.8	8	+16.2±13.8	8
6.35	+13.2 4.6	31	+ 1.5 8.7	6	+ 1.5 8.7	6
6.75	+ 9.0 4.0	43	+ 6.0 7.1	20	+ 6.0 7.1	20
7.15	-10.1 3.3	39	-18.4 3.3	25	-18.4 3.6	23
7.45	+10.4 3.2	28	- 2.4 6.2	16	- 2.4 6.2	16
7.65	- 2.6 2.9	39	-15.4 4.7	21	-15.4 4.7	21
7.85	+ 1.2 1.7	57	+ 1.0 2.0	44	+ 1.1 2.3	39
8.0	- 1.6 1.3	48	- 1.4 1.3	46	- 0.7 1.6	32
8.1	- 4.7 0.7	81	- 4.7 0.7	80	- 5.4 0.7	64
8.2	- 6.9 0.7	83	- 6.9 0.7	83	- 6.7 0.7	64
8.3	- 1.8 0.9	86	- 1.8 0.9	86	- 1.0 1.1	67
8.4	- 2.3 1.2	68	- 2.2 1.2	61	- 2.4 1.5	48
8.5	+ 3.0 2.6	32	+ 4.5 2.7	27	+ 3.6 3.4	19
8.65	- 4.5 1.7	39	- 4.7 1.7	38	- 3.2 1.4	32
8.85	- 6.9 3.4	34	- 6.4 4.0	26	- 5.0 3.9	25
9.15	- 0.1 2.0	59	+ 2.0 2.5	37	+ 2.4 2.5	36
9.55	- 6.9 2.0	44	- 7.6 2.0	32	- 7.5 2.1	31
10.30	- 5.2±3.4	44	- 2.6±4.5	24	- 2.6±4.5	24

quadrant, the stars are moving more rapidly than in the Schmidt (1956) model, and would give rise to excess positive radial velocities. In the 2nd quadrant, the observed radial velocities would be less negative than predicted; in the 3rd quadrant, less positive, and in the 4th quadrant, more negative. Deviations of this sort from the double sine can be easily noted in the radial-velocity analysis of early-type stars by Feast and Thackeray (1958, Figs. 3, 4, and 5) for the 1st, 3rd, and 4th quadrants. The excess negative velocities in the 3rd quadrant have already been noted in Sec. III of this paper.

The value of Oort's constant A , for the solar vicinity, would be difficult to evaluate uniquely, for such a rotation curve. In the solar vicinity, A is given by

$$A = \frac{1}{2}[(\Theta_0/R_0) - (d\Theta/dR)_0]. \quad (27)$$

For stars toward the center of the galaxy, $-d\Theta/dR$ is of the order of +20 km/sec per kpc; for stars toward the anticenter it is close to zero. Hence for the adopted values of Θ_0 and R_0 , values of A ranging from 23 km/sec per kpc to 13 km/sec per kpc could be expected, depending upon the distribution in galactic longitude of the stars under study. Such widely divergent values of A have actually been obtained in recent studies (Weaver 1961; Feast and Thackeray 1958, and references therein). An analysis is now being made to determine the value of Oort's constants A and B for the stars in Table IV.

VI. COMPONENT OF VELOCITY RADIAL FROM THE CENTER OF THE GALAXY

For 888 stars, the components of motion radial from the center of the galaxy have been combined into one mean curve which is shown in the upper plot of Fig. 5. The circles represent the weighted means; the vertical lines indicate the weighted probable error, computed

from Eq. (20). These values of $\langle \Pi \rangle$ are listed in Table VII, along with $\langle \Pi \rangle$ determined from several other solutions.

The slope of the $\langle \Pi \rangle$ vs R curve is independent of the value chosen for \dot{x}_0 , but the absolute values of $\langle \Pi \rangle$ are not. For the adopted value, $\dot{x}_0=+10.5$ km/sec, the values in Fig. 5 result; if $\dot{x}_0=0$ had been used, the horizontal axis would be located at $\rho=-10$ km/sec in Fig. 5.

The value of $\langle \Pi \rangle$ is a maximum for stars closest to the center, and decreases with a fairly uniform slope of about 5 km/sec per kpc. Interestingly, this is close to the value one might infer from radio observations. Near the center of the galaxy, the gas is observed to have an expansion velocity of about 50 km/sec (van Woerden *et al.* 1957; Rougoor and Oort 1960). At the position of the sun, the expansion velocity is about 7 km/sec, according to Kerr (1960, 1961).

Again, it is necessary to investigate the effects of systematic observational errors on the determined $\langle \Pi \rangle$ curve.

(a) *The MK luminosity calibration.* For a constant error ΔM in the absolute magnitude calibration, $\Delta \Pi$ can be found from Eqs. (7), (8), (12), and (22):

$$\Delta \Pi \approx -0.46r\Delta M \sin l^{\text{II}}$$

$$\times \left[(A \cos 2l^{\text{II}} + B) \left(1 + \frac{2r}{R} \cos l^{\text{II}} \right) + \frac{\Theta_0}{R} \right]. \quad (28)$$

For $l^{\text{II}}=0^\circ$ or 180° , $\Delta \Pi$ is zero. For $l^{\text{II}}=90^\circ$ and 270° , $\sin l^{\text{II}}=\pm 1$, and

$$\Delta \Pi \approx \mp 0.46r\Delta M (-A + B + \Theta_0/R). \quad (29)$$

This last expression is approximately equal to zero, because $-A + B \approx \Theta_0/R$ for $R \approx R_0$. Moreover, the mean value $\langle \Delta \Pi \rangle$ will equal zero at every R for a uniform

distribution of stars, because the mean at each R will include equal values of positive and negative $\sin\Pi^{\text{II}}$.

(b) *The proper-motion system.* For proper motions on a mean N30-FK4 system, the corrections in Table V were applied. From Eqs. (7), (8), and (12),

$$\Delta\Pi \approx \kappa r \Delta\mu_1 \sin\Pi^{\text{II}} [1 + (r/R) \cos\Pi^{\text{II}}]. \quad (30)$$

The value of $\langle\Pi\rangle$ for each point $6.2 \leq R \leq 7.8$ kpc is increased about +5 km/sec on the mean proper-motion system. There is no change in $\langle\Pi\rangle$ for $R > 7.8$ kpc.

(c) *Radial velocities.* If the radial velocities are in error by a constant $\Delta\rho$,

$$\Delta\Pi \approx \Delta\rho [-\cos\Pi^{\text{II}} + (r/R) \sin^2\Pi^{\text{II}}]. \quad (31)$$

For $\Delta\rho$ positive, points toward the center will be lowered, those toward the anticenter will be raised. In the solution for $\langle\Pi\rangle$ with all Lick radial-velocity stars deleted, the six inner points are decreased; there is no significant change in $\langle\Pi\rangle$ for $R > 7.8$ kpc. In the solution shown in Fig. 5, the Lick stars have been given lower weight than non-Lick stars.

If the inner points of the $\langle\Pi\rangle$ curve (Fig. 5) are raised 5 km/sec for the mean N30-FK4 proper-motion system, and lowered about the same amount due to corrections to the Lick radial velocities, there is little change from the values shown. Stars toward the center of the galaxy are receding from the center, and approaching the sun. Stars toward the anticenter are approaching the center (for the choice of $\dot{x}_0 = +10$ km/sec) and hence approaching the sun. Stars in the center and anticenter directions would thus appear to be contracting toward the observer. Evidence for a contraction of interstellar gas and young stars in the galactic plane, i.e., a negative K term, has been noted and summarized by Feast and Thackeray (1958). The negative slope of the $\langle\Pi\rangle$ curve found here would produce a negative K term in the analysis of the radial velocities; the two phenomena are equivalent (Trumpler and Weaver 1953, p. 583).

Finally, mention should be made of the value $\langle\Pi\rangle = -7$ km/sec at $R = 8.2$ kpc. A value of $\dot{x}_0 = +10.5$ km/sec has been adopted; this is equivalent to a value of $\Pi_0 = -10.5$ km/sec. The computed value of \dot{x}_e for each star has been modified by this amount. Hence a value of $\langle\Pi\rangle$ of about -7 km/sec at $R = 8.2$ kpc is principally a reflection of the adopted component of solar motion in the Π direction. Thus, with respect to all the stars in the sample in the ring at $R = 8.2$ kpc, the sun has almost no component of motion in the Π (the $-\dot{x}$) direction. If the entire ring of stars is expanding from the center of the galaxy, as Kerr (1960, 1961) has postulated for the gas, such an expansion cannot be deduced from this analysis. All that can be inferred is that the motion of the sun in the Π direction is similar to the $\langle\Pi\rangle$ motion of all the stars with $R = 8.2$ kpc.

VII. CONCLUSIONS

In this paper, a catalogue of 1440 early-type stars in the galactic disk and within 3 kpc of the sun has been presented. Photometric data and radial velocities are tabulated for all stars in Table I. For 898 of these stars, proper motions on the N30 system are available and listed in Table IV. From a study of the distribution in the galactic plane, distribution of radial velocities, and galactic space motions, the following conclusions are presented.

(1) About 5% of all O-B5 stars within 3 kpc of the sun are included in this study. No published radial velocities were found for other O-B5 stars within this distance. The projection on the galactic plane of these stars alone (Fig. 1) does not indicate any pronounced spiral structure. This may be due to incompleteness of the sample in the regions where interstellar hydrogen has a maximum density. In conjunction with results from earlier discussions of spiral structure, the Carina-Cygnus arm, the Orion spur, and the Sagittarius extension are apparent.

It is assumed that the stars in Table I constitute a representative sample of the nearby early-type stars in the galactic disk. This may not be the case, if highly reddened stars in regions of large interstellar absorption have not been observed. If these undetected early-type stars are stars of lower velocity, which have not yet emerged from the regions of high gas density in which they were formed, then the motions of the stars in Table I might be larger than the general disk population of early-type stars. Such effects can not be considered at present.

(2) There is good qualitative agreement between the stellar radial-velocity distributions grouped in 5° longitude zones, and the corresponding 21-cm line profiles, in most directions in the galactic plane (Fig. 3). In many cases, however, the stellar velocities show a larger spread in radial velocity than that predicted by the radio model of the galaxy. This could be accounted for by random stellar radial velocities up to 20 km/sec; alternatively, the adopted parameters of the radio model could be altered. A value of $R_0 = 10$ kpc, rather than the commonly adopted $R_0 = 8.2$ kpc, would improve the agreement between the stellar and radio radial-velocity distributions in some longitude zones.

(3) For 888 stars, the rotational velocity component about the center of the galaxy has been computed, and a mean curve derived (Fig. 5). Toward the center of the galaxy, the computed curve lies about 15 km/sec above the radio rotation curve (Schmidt 1956). For $R > 8$ kpc, the rotation curve is approximately flat. The decrease in rotational velocity expected for Keplerian orbits is not found. It is shown that systematic observational errors will not account for the shape of the curve.

(4) With a rotation curve of the computed form, it is evident that the value of Oort's constant A will vary, depending on the longitude distribution of the sample of

stars under study. This may account in part for the widely divergent values of A found in recent work (Weaver 1961; Feast and Thackeray 1958). For a sample with most stars toward the center of the galaxy, a large value of A would result from the large gradient, $d\Theta/dR$. For stars principally toward the anticenter, a small value of A would be obtained.

(5) The velocity component radial from the center of the galaxy shows a large scatter for individual stars. In the mean, the curve has a negative slope of about -5 km/sec per kpc. Stars toward the center show a velocity of recession from the center; stars with large R indicate a slight velocity of approach toward the center, for the conventional choice of solar motion. This substantiates the observation of Feast and Thackeray (1958) of a contraction of matter in the galactic plane, and agrees well with the expansion postulated for interstellar neutral hydrogen.

This paper is the first of several studies of early-type stars, based on data contained in Tables I and IV. Later papers will consider the angular velocity of the sun about the center of the galaxy, the distribution of absorbing matter in the galactic plane, and the values of Oort's constants A and B determined from the motions of these stars.

ACKNOWLEDGMENTS

This work was done as a class problem in a course on Stellar Dynamics. The senior author would like to thank Martin F. McCarthy, S. J., visiting astronomer at Georgetown College Observatory from the Vatican Observatory, for many stimulating discussions. Special thanks are due Robert J. Rubin. Many of the ideas developed in this paper arose in conversations with him.

REFERENCES

- Bahng, J. D., Code, A. D., and Whitford, A. E. 1957, *Sky and Telescope* **16**, 529.
 Barbier, M., and Boulon, J. 1959, *J. Obs.* **43**, 69.
 Beals, C. S. 1955, *Publ. Dominion Astrophys. Obs.* **IX**, 1.
 Beer, A. 1961, *Monthly Notices Roy. Astron. Soc.* **123**, 191.
 Bertiau, F. C., S. J. 1958, *Astrophys. J.* **128**, 533.
 Blaauw, A. 1956, *ibid.* **123**, 408.
 Blaauw, A., Gum, C. S., Pawsey, J. L., and Westerhout, G. 1959, *ibid.* **130**, 702.
 Blanco, V. M., and Lennon, C. J. 1961, *Astron. J.* **66**, 524.
 Bok, B. J. 1959, *Observatory* **79**, 58.
 Boss, B. 1937, *General Catalogue of 33 342 Stars for Epoch 1950* (Carnegie Institution of Washington, Washington, D. C.).
 Boulon, J., Duflot, M., and Fehrenbach, Ch. 1958, *Publ. Obs. Haute-Provence* **4**, No. 34.
 Boulon, J., and Fehrenbach, Ch. 1959, *ibid.* **4**, No. 55.
 Cape Observatory, *Annals of the* 1954, **XVII**. 1954, **XVIII**. 1954, **XIX**. 1958, **XX**.
 Duflot, M., and Fehrenbach, Ch. 1956, *Publ. Obs. Haute-Provence* **3**, No. 49.
 —. 1957, *ibid.* **4**, No. 12.
 Eggen, O. J. 1961, *Roy. Obs. Bull.* **41**, 245.
 Evans, D. S., Menzies, A., and Stoy, R. H. 1959, *Monthly Notices Roy. Astron. Soc.* **119**, 638.
 Feast, M. W., and Thackeray, A. D. 1958, *ibid.* **118**, 125.
 Feast, M. W., Thackeray, A. D., and Wesselink, A. J. 1955, *Mem. Roy. Astron. Soc.* **LXVIII**, 51.
 —. 1957, *ibid.* **LXVIII**, 1.
 Hardorp, J., Rohlf, K., Slettebak, A., and Stock, J. 1959, *Luminous Stars in the Northern Milky Way* (Hamburg-Bergedorf), Vol. I.
 Hiltner, W. A. 1956, *Astrophys. J. Suppl.* **2**, 389.
 Hiltner, W. A., and Johnson, H. L. 1956, *Astrophys. J.* **124**, 367.
 van de Hulst, H. C. 1958, *Rev. Modern Phys.* **30**, 913.
 van de Hulst, H. C., Muller, C. A., and Oort, J. H. 1954, *Bull. Astron. Inst. Neth.* **XII**, 117.
 Johnson, H. L. 1958, *Lowell Obs. Bull.* **4**, 37.
 Johnson, H. L., and Hiltner, W. A. 1956, *Astrophys. J.* **123**, 267.
 Johnson, H. L., and Iriarte, B. 1958, *Lowell Obs. Bull.* **4**, 47.
 Kahn, F. D. 1960, *Die Entstehung von Sternen* (Springer-Verlag, Berlin), p. 154.
 Kerr, F. J. 1960, *Nature* **188**, 216.
 —. 1961, *Astron. J.* **66**, 47.
 Kerr, F. J., Hindman, J. V., and Gum, C. S. 1959, *Australian J. Phys.* **12**, 270.
 Kopylov, I. M. 1959, *Ann. d'Astrophys. Suppl.* **8**, 41.
 Kwee, K. K., Muller, C. A., and Westerhout, G. 1954, *Bull. Astron. Inst. Neth.* **XII**, 220.
 Mayall, N. U. 1951, *Publ. Obs. Univ. Mich.* **10**, 19.
 McCuskey, S. W. 1956, *Astrophys. J.* **123**, 458.
 Morgan, H. R. 1933, *Publ. U. S. Naval Obs. 2nd Ser.* **XIII**, 163.
 —. 1952, *Astron. Papers Am. Ephemeris and Naut. Almanac* **XIII**, part III.
 —. 1956, *Astron. J.* **61**, 90.
 Morgan, H. R., and Oort, J. H. 1951, *Bull. Astron. Inst. Neth.* **XI**, 379.
 Morgan, W. W., Harris, D. L., and Johnson, H. L. 1953, *Astrophys. J.* **118**, 92.
 Muller, C. A., and Westerhout, G. 1957, *Bull. Astron. Inst. Neth.* **XIII**, 151.
 Munch, G., and Munch, L. 1960, *Astrophys. J.* **131**, 253.
 Oosterhoff, P. Th. 1951, *Bull. Astron. Inst. Neth.* **XI**, 299.
 Petrie, R. M. 1955, *Publ. Dominion Astrophys. Obs.* **IX**, 251.
 —. 1956, *Vistas in Astronomy*, edited by A. Beer (Pergamon Press, London and New York), Vol. II, p. 1346.
 —. 1958, *Monthly Notices Roy. Astron. Soc.* **118**, 80.
 —. 1962, *ibid.* **123**, 501.
 Petrie, R. M., and Moyle, B. N. 1956, *Publ. Dominion Astrophys. Obs.* **X**, 287.
 Reiz, A. 1957, *Ann. Lund Obs.* **14**, 1.
 Roberts, M. S. 1957, *Publ. Astron. Soc. Pacific* **69**, 59.
 Rougoor, G. W., and Oort, J. H. 1960, *Proc. Natl. Acad. Sci. U. S.* **46**, 1.
 Rubin, V., Burley, J., Kiasatpoor, A., Klock, B., Pease, G., Rutscheidt, E., and Smith, C. 1962, *Astron. J.* **67**, 281.
 Schmidt, M. 1956, *Bull. Astron. Inst. Neth.* **XIII**, 15.
 —. 1957, *ibid.* **XIII**, 247.
 Sharpless, S. 1952, *Astrophys. J.* **116**, 251.
 Stock, J., Nassau, J. J., and Stephenson, C. B. 1960, *Luminous Stars in the Northern Milky Way* (Hamburg-Bergedorf), Vol. II.
 Stoy, R. H. 1961, *Cape Memo.* **12**, Royal Obs., Cape of Good Hope.
 Trumpler, R. J., and Weaver, H. F. 1953, *Statistical Astronomy* (University of California Press, Berkeley and Los Angeles).
 Weaver, H. 1961, *Publ. Astron. Soc. Pacific* **73**, 88.
 Westerhout, G. 1957, *Bull. Astron. Inst. Neth.* **XIII**, 201.
 Wilson, R. E. 1953, *General Catalogue of Stellar Radial Velocities* (Carnegie Institution of Washington, Washington, D. C.).
 van Woerden, H., Rougoor, G. W., and Oort, J. H. 1957, *Compt. rend.* **244**, 1691.
 Woolley, R. v. d. R., and Eggen, O. J. 1958, *Observatory* **78**, 149.
 Yale University, *Trans. Astron. Obs. of* **11**, 1939. **12**, 1940. **13**, 1943. **14**, 1943. **16**, 1945. **17**, 1945. **18**, 1947. **19**, 1948. **20**, 1949. **21**, 1950. **22**, 1950. **24**, 1953. **25**, 1954. **26**, 1959. **27**, 1959.